


Comparative analysis of tangential flow filtration and ultracentrifugation, both combined with subsequent size exclusion chromatography, for the isolation of small extracellular vesicles

Kekoolani S. Visan¹  | Richard J. Lobb^{1,2} | Sunyoung Ham¹ | Luize G. Lima¹ | Carlos Palma³ | Chai Pei Zhi Edna¹ | Li-Ying Wu^{1,4} | Harsha Gowda⁵ | Keshava K. Datta^{5,6} | Gunter Hartel⁷ | Carlos Salomon^{3,8} | Andreas Möller¹

¹Tumour Microenvironment Laboratory, QIMR Berghofer Medical Research Institute, Herston, QLD, Australia

²Centre for Personalized Nanomedicine, Australian Institute for Bioengineering and Nanotechnology (AIBN), The University of Queensland, Brisbane, QLD, Australia

³Exosome Biology Laboratory, Faculty of Medicine and Biomedical Sciences, Centre for Clinical Diagnostics, University of Queensland Centre for Clinical Research, Royal Brisbane and Women's Hospital, The University of Queensland, Brisbane, QLD, Australia

⁴School of Biomedical Sciences, Faculty of Health, Queensland University of Technology, Brisbane, QLD 4059, Australia

⁵Cancer Precision Medicine Laboratory, QIMR Berghofer Medical Research Institute, Herston, QLD, Australia

⁶Proteomics and Metabolomics Platform, La Trobe University, Bundoora, VIC, Australia

⁷Statistics Unit, QIMR Berghofer Medical Research Institute, Herston, QLD, Australia

⁸Departamento de Investigación, Postgrado y Educación Continua (DIPEC), Facultad de Ciencias de la Salud, Universidad del Alba, Santiago, Chile

Correspondence

Richard J. Lobb, Australian Institute for Bioengineering and Nanotechnology, The University of Queensland, QLD 4072, Australia.
Email: richard.lobb@uq.edu.au

Andreas Möller, Locked Bag 2000 Royal Brisbane Hospital, QLD 4029, Australia.
Email: andreas.moller@qimrberghofer.edu.au

Funding information

National Health and Medical Research Council, Grant/Award Numbers: 1114013, APP1185907; National Breast Cancer Foundation Australia, Grant/Award Number: IIRS-18-159

Abstract

Small extracellular vesicles (sEVs) provide major promise for advances in cancer diagnostics, prognostics, and therapeutics, ascribed to their distinctive cargo reflective of pathophysiological status, active involvement in intercellular communication, as well as their ubiquity and stability in bodily fluids. As a result, the field of sEV research has expanded exponentially. Nevertheless, there is a lack of standardisation in methods for sEV isolation from cells grown in serum-containing media. The majority of researchers use serum-containing media for sEV harvest and employ ultracentrifugation as the primary isolation method. Ultracentrifugation is inefficient as it is devoid of the capacity to isolate high sEV yields without contamination of non-sEV materials or disruption of sEV integrity. We comprehensively evaluated a protocol using tangential flow filtration and size exclusion chromatography to isolate sEVs from a variety of human and murine cancer cell lines, including HeLa, MDA-MB-231, EO771 and B16F10. We directly compared the performance of traditional ultracentrifugation and tangential flow filtration methods, that had undergone further purification by size exclusion chromatography, in their capacity to separate sEVs, and rigorously characterised sEV properties using multiple quantification devices, protein analyses and both image and nano-flow cytometry. Ultracentrifugation and tangential flow filtration both enrich consistent sEV populations, with similar size distributions of particles ranging up to 200 nm. However, tangential flow filtration exceeds ultracentrifugation in isolating significantly higher yields of sEVs, making it more suitable for large-scale research applications. Our results demonstrate that

This is an open access article under the terms of the [Creative Commons Attribution-NonCommercial-NoDerivs License](https://creativecommons.org/licenses/by-nc-nd/4.0/), which permits use and distribution in any medium, provided the original work is properly cited, the use is non-commercial and no modifications or adaptations are made.

© 2022 The Authors. *Journal of Extracellular Vesicles* published by Wiley Periodicals, LLC on behalf of the International Society for Extracellular Vesicles.

tangential flow filtration is a reliable and robust sEV isolation approach that surpasses ultracentrifugation in yield, reproducibility, time, costs and scalability. These advantages allow for implementation in comprehensive research applications and downstream investigations.

KEYWORDS

cell culture, extracellular vesicles, isolation, tangential flow filtration

1 | INTRODUCTION

Extracellular vesicles (EVs) play a crucial role in the promotion, progression and sustenance of cancer due to their autocrine and paracrine signalling behaviour (Kalluri & Lebleu, 2020; Möller & Lobb, 2020). In particular, interest in the research of small EVs (sEVs), ranging from approximately 30 to 200 nm in size, has surged over the recent years (Li et al., 2019; Möller & Lobb, 2020). These cell-derived, bilipid-layered particles contain complex cargo and are highly stable and present in all bodily fluids, hence are great candidates as biomarkers for the detection of cancer (Kalluri & Lebleu, 2020; Möller & Lobb, 2020; Visan et al., 2022). Additionally, sEVs effectively function in intercellular communication, thus contributing to cancer pathogenesis and cancer microenvironmental processes, as well as providing great promise for clinical translation (Kalluri & Lebleu, 2020; Möller & Lobb, 2020; Visan et al., 2020). However, due to the fast-paced expansion of sEV-based research and a lack of general consensus, a major issue in the field is the need for appropriate isolation methods (Royo et al., 2020).

Centrifuge-based ultrafiltration in combination with size exclusion chromatography is a highly efficient method of sEV isolation, with significant levels of yield, quality, purity, time efficiency and reproducibility (Lobb et al., 2015). However, this method relies on cells being grown in serum-free media. Most cell types require foetal bovine serum (FBS) for nutrient supplementation and optimal growth in their media (Eitan et al., 2015), and since lack of serum is a potential stress-inducer, growing cells in FBS-free media could falsify sEV content and function analysis (Abramowicz et al., 2018; Li et al., 2015). Serum-containing media is used by the majority of researchers for culturing cells for the purpose of sEV isolation (Gardiner et al., 2016; Royo et al., 2020; Sciences BCL, 2019). Hence there is a strong demand for developing a protocol capable of sEV isolation from cells grown in serum-containing media.

Most researchers use ultracentrifugation-based methodology for the isolation of sEVs from cell culture conditioned media (Gardiner et al., 2016; Royo et al., 2020; Sciences BCL, 2019; Van Deun et al., 2017). Although ultracentrifugation is the most commonly used technique, there are several problems associated with its use (Gardiner et al., 2016; Nordin et al., 2019). Repeated rounds of ultracentrifugation can disrupt the structural and biological integrity of sEVs, cause aggregation, result in co-isolation of contaminating non-EV particles and/or proteins, as well as produce suboptimal sEV yield (Heath et al., 2018; Lobb et al., 2015; Nordin et al., 2019). This can impact downstream applications and their interpretation, including analysis of sEV composition and structure (Lamparski et al., 2002). The disadvantages of ultracentrifugation have driven researchers in both academia and industry to implement gentle isolation approaches, hence the rise in the use of tangential flow filtration and size exclusion chromatography (Royo et al., 2020).

Tangential flow filtration is a system that concentrates and filters out particles using a cross-flow filtration principle. Typically, ultrafiltration devices use dead-end filtration, where media is applied perpendicular to the membrane in order to flux the entire volume at once (Van der Bruggen, 2018). Decreased membrane permeability and resulting increased operation times and inefficiencies can arise in those dead-end filtration systems (Van der Bruggen, 2018). In contrast, tangential flow filtration applies the media parallel to the membrane, as well as through the membrane, preventing molecule accumulation and membrane fouling, and does so until the entire volume has been fluxed (Figure 1A). The application of size exclusion chromatography is prevalent across laboratories worldwide (Royo et al., 2020) due to its gentle nature and efficiency for eliminating contaminating materials (Baranyai et al., 2015; Guan et al., 2020; Lobb et al., 2015; Stam et al., 2021). Based on the growth in the use of isolation techniques that preserve EV integrity and prevent EV aggregation (Royo et al., 2020), as well as recent reports of the application of tangential flow filtration (Andrade et al., 2021; Binder et al., 2021; Busatto et al., 2018; El Baradie et al., 2020; Haraszti et al., 2018; Heine-mann et al., 2014) coupled with size exclusion chromatography (Coenen-Stass et al., 2019; Corso et al., 2017; Gomes et al., 2022; Mcnamara et al., 2018; Nordin et al., 2019; Wolf et al., 2022), it can be anticipated that this combinatorial method may become standard for many laboratories in the near future.

Here, we present a complete analysis of an optimised protocol for the isolation of sEVs from cells grown in serum-containing media based on tangential flow filtration and subsequent size exclusion chromatography. The coupling of ultracentrifugation and size exclusion chromatography is a common technique employed by EV researchers (Alameldin et al., 2021; Koh et al., 2018; Stam et al., 2021). For this reason, it was important to comprehensively assess sEVs isolated by ultracentrifugation and tangential flow filtration, in conjunction with size exclusion chromatography. Hence our tangential flow filtration protocol was rigorously compared to the commonly used ultracentrifugation method after size exclusion chromatography purification, based

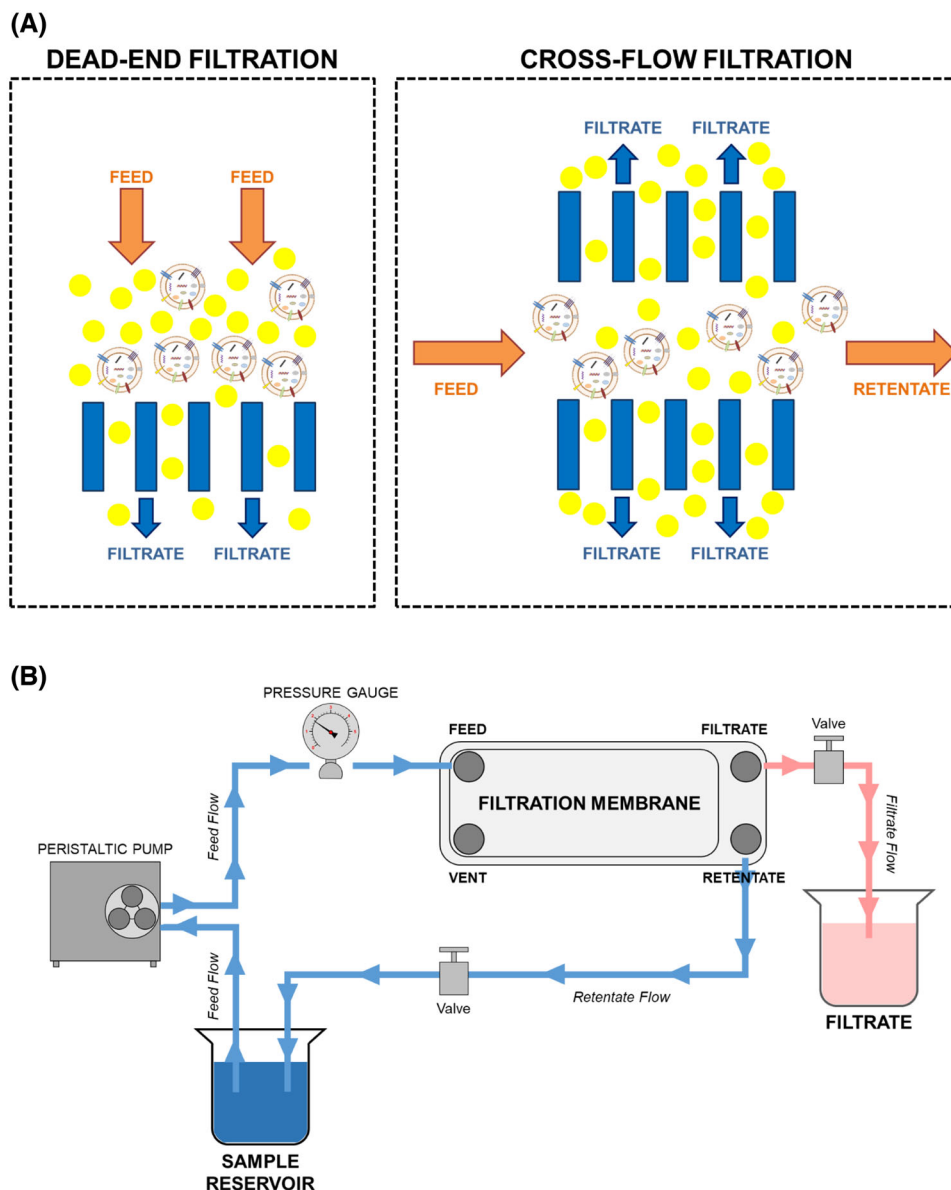


FIGURE 1 The principle of tangential flow filtration. (A) Representation of dead-end filtration and cross-flow filtration. (B) A schematic illustration of a tangential flow filtration system. Using a peristaltic pump, CCM travels from the sample reservoir, through to the filtration membrane, where molecules smaller than the molecular weight cut-off are filtered out via the filtrate flow, and molecules larger than the molecular weight cut-off are retained and recirculated back to the sample reservoir via the retentate flow. The pressure gauge is used to maintain appropriate flow rates, and valves are used to redirect flow for filtration and recirculation steps. CCM: cell culture conditioned media

on factors such as yield, purity, quality, specificity, costs, time requirements and reproducibility across different cell lines and species. We conclude that tangential flow filtration is advantageous to ultracentrifugation and requires minimal infrastructure, making it a prospective primary isolation method to be used in a wider variety of laboratory settings, for the isolation of sEVs from serum-containing media.

2 | MATERIALS AND METHODS

2.1 | Cell culture

Human cervical cancer cell line HeLa, and human breast cancer cell line MDA-MB-231, were purchased from American Type Culture Collection (ATCC). Murine breast cancer cell line EO771 (Ham et al., 2018), and murine melanoma cell line B16F10 (Möller et al., 2009; Sceneay et al., 2012), were described previously. Cells tested negative for mycoplasma contamination. Human

cell line authentication was carried out by in-house short tandem repeat (STR) profiling. Cells were maintained in high-glucose Dulbecco's Modified Eagle Medium (DMEM) supplemented with 5% FBS, 100 U/ml penicillin and 100 mg/ml streptomycin (Gibco, CA, USA) and grown in an incubator at 37°C with 5% CO₂. For sEV isolation, cells were seeded into 150 mm x 25 mm dishes at a concentration of 1.5×10^6 cells/dish for HeLa, MDA-MB-231 and B16F10 cell lines, and 1×10^6 cells/dish for the EO771 cell line. After overnight adhesion, cells were washed with Dulbecco's phosphate buffered saline (PBS) and conditioned in DMEM containing 5% EV-depleted FBS, generated as described (Théry et al., 2006), for 48 h (15 ml/dish). Cell culture conditioned media were collected and centrifuged at $500 \times g$ for 10 min using a Beckman Coulter Allegra X-15R, in order to remove detached cells and large debris. Supernatant was collected and filtered through 0.22 μm filters (Merck Millipore) to remove any other large particle contaminants, to clarify the conditioned media.

2.2 | Ultracentrifugation

Clarified cell culture conditioned media (depleted of detached cells, large debris and large particle contaminants) were centrifuged in a Beckman Coulter Optima XPN-80 Ultracentrifuge at $100,000 \times g$ at 4°C for 120 min, with a 50.2 Ti rotor (k-factor: 157.7) to pellet EVs. The supernatant was carefully removed, and crude sEV pellets were resuspended in 1 ml of ice-cold PBS and pooled. For cell lines MDA-MB-231, B16F10 and EO771, a second round of ultracentrifugation was carried out using the Beckman Coulter Optima XPN-80 Ultracentrifuge at $100,000 \times g$ at 4°C for 120 min, with a 50.2 Ti rotor (k-factor: 157.7). For the HeLa cell line, a second round of ultracentrifugation was carried out using the Hitachi Himac CS150NX Ultracentrifuge at $100,000 \times g$ at 4°C for 90 min, with an S55A2 rotor (k-factor: 40). The resulting pellets were resuspended in PBS (volumes ranged from 100 to 300 μl depending on pellet size) and stored at -80°C .

2.3 | Tangential flow filtration

Clarified cell culture conditioned media (depleted of detached cells, large debris and large particle contaminants) was concentrated using sterile Minimate Tangential Flow Filtration Capsules with 300, 500 or 1000 kDa Omega Membranes (Pall Corporation). Filtration was carried out using a MASTERFLEX Console Analog L/S Pump Drives (Model No. 77521-47) peristaltic pump.

For concentration of buffers and cell culture conditioned media, the speed of the peristaltic pump was adjusted to maintain a feed pressure (P_{Feed}) of 30 psi, retentate pressure ($P_{\text{Retentate}}$) of 25 psi and filtrate pressure (P_{Filtrate}) of 0 psi, in order to preserve the integrity of the filter. The transmembrane pressure (TMP) was maintained at 2.5 psi (according to $\text{TMP} = ((P_{\text{Feed}} - P_{\text{Retentate}}) / 2) - P_{\text{Filtrate}}$). Cell culture conditioned media were added to the reservoir and concentrated at a rate of 10–15 ml/min, 6–9 ml/min, 5–8 ml/min and 6–9 ml/min for HeLa, MDA-MB-231, EO771 and B16F10 cell lines, respectively, to a final volume of 10 ml (Figure 1B). Concentration was followed by buffer recirculation and diafiltration using an equal volume of PBS as the original conditioned media. PBS was added to the reservoir and recirculated through the system for 10 min to detach any impurities and/or EVs that may be lodged in the filter membrane. After recirculation, sample was concentrated to a final volume of 10 ml. Recirculation/diafiltration was repeated for a total of three times. The final 10 ml volume was recirculated for 10 min and collected from the reservoir. Another 10 ml of PBS was added to the reservoir, recirculated through the filter for 10 min, and then collected. This step was repeated a final time, thus the recirculation of 10 ml PBS volumes was conducted a total of three times. The final 30 ml volume was further concentrated using a Centricon Plus-70 Centrifugal Filter (Ultracel-PL Membrane, 100 kDa) device by centrifugation at $3000 \times g$ at 4°C using an Allegra X-15R centrifuge. The concentrate was recovered by a reverse spin at $1000 \times g$ at 4°C for 2 min. To ensure thorough flux, 1 ml of PBS was added to the Centricon Plus-70 Centrifugal Filter and concentrated for 2 min by centrifugation at $3000 \times g$ at 4°C using an Allegra X-15R centrifuge. The concentrate was recovered by a reverse spin at $1000 \times g$ at 4°C for 2 min. This step was repeated for a total of three times. The final volume was diluted at 1:3 ratio in PBS and stored at -80°C .

All Minimate Tangential Flow Filtration Capsules with Omega Membranes (Pall Corporation) are reusable and require cleaning with appropriate buffers. Prior to processing the cell culture conditioned media, the filter was washed with sterile PBS (pH 7.4), 20% EtOH, then again with sterile PBS. Post-processing, membranes were washed with sterile PBS and 0.1 M NaOH, and then stored at 4°C.

2.4 | Size exclusion chromatography

Size exclusion qEV columns (qEVoriginal, 70 nm) were purchased from Izon Science Ltd and stored in 0.1% sodium azide at 4°C. EV (isolated by ultracentrifugation or tangential flow filtration) aliquots of 500 μl were overlaid on the qEV columns followed by elution with PBS, and 500 μl fractions were collected. The EV-containing fractions (fractions 7–10) were pooled and concentrated

in Amicon Ultra-4 10 kDa centrifugal filter units by centrifugation at $4000 \times g$ at 4°C to a final volume of approximately $200 \mu\text{l}$, using an Allegra X-15R centrifuge (Lobb et al., 2015). The final sEV samples were collected and stored at -80°C until use.

2.5 | Tunable resistive pulse sensing (TRPS)

Tunable Resistive Pulse Sensing (qNano, Izon Science Ltd) was utilised as described previously (Wen et al., 2019) to analyse the concentration and size distribution of the particles isolated, using NP150 nanopores at a 45.50-mm stretch. 110-nm carboxylated polystyrene beads (1.2×10^{13} particles/ml) were used to standardise concentration and size. Quantification of total particle yield and size distribution was normalised to the starting volume of cell culture conditioned media, as well as the final volume of sEV sample (either before or after size exclusion chromatography).

2.6 | Nanoparticle tracking analysis (NTA)

2.6.1 | Zeta view

Prior to sample measurement using ZetaView (Particle Metrix, Germany) and its corresponding software (version 8.05.12 SP1), several parameters were set, including: temperature, $\sim 25^{\circ}\text{C}$; pH, 7.4; frame rate, 30 frames per second; and shutter speed of 100. All samples were diluted in PBS to 1 ml, which was then loaded into the cell (Cell# ZNTA_19-424) and measured by the scanning of 11 different positions for two cycles. After measurement, video recordings were analysed by the ZetaView software (version 8.05.12 SP1) and parameters were set for maximum area: 1000; minimum area: 10; maximum brightness: 255; minimum brightness: 30. Analyses were conducted in the scattered light mode with a laser wavelength of 488 nm. Quantification of total particle yield and size distribution was normalised to the starting volume of cell culture conditioned media, as well as the final volume of sEV sample (either before or after size exclusion chromatography).

2.6.2 | NanoSight

NanoSight NS500 (NanoSight NTA 3.1 Nanoparticle Tracking and Analysis Release Version Build 3.1.46) was used following the manufacturer's instructions, and as previously described (Salomon et al., 2014). Briefly, samples were processed in duplicate and diluted with PBS over a range of concentrations to obtain between 10 and 100 particles per image (optimal: ~ 50 particles per image) before the analysis with NanoSight. Samples were added into the chamber (temperature: 25°C , and viscosity: 0.89 cP) and the camera level set to obtain an image that had sufficient contrast to clearly identify particles while minimising background noise for video recording (camera level: 13, and capture duration: 30 s). After that, the captured videos (three videos per sample) were processed and analysed. A combination of high shutter speed (600) and gain (250), followed by manual focusing, enabled optimum visualisation of a maximum number of vesicles. A minimum of 200 tracks completed per video was included as duplicates. Post-acquisition settings were optimised and kept constant between samples (frames processed: 1496 of 1496; frames per second: 30; camera shutter: 20 ms; calibration: 139 nm/pixel; blur: 3×3 ; detection threshold: 10; min track length: auto; min expected size: auto), and each video was then analysed to give the mean, mode, and median particle size together with an estimate of the number of particles. An Excel spread sheet (Microsoft Corp., Redmond, Washington) was automatically generated, showing the concentration at each particle size bin. Quantification of total particle yield and size distribution was normalised to the starting volume of cell culture conditioned media, as well as the final volume of sEV sample (either before or after size exclusion chromatography).

2.7 | Transmission electron microscopy

SEVs were visualised using transmission electron microscopy, as previously described (Salomon et al., 2017). Briefly, sEVs were fixed in 3% (w/v) glutaraldehyde, and 2% paraformaldehyde in cacodylate buffer (pH 7.3). The fixed sEVs ($5 \mu\text{l}$) were applied to a continuous carbon grid and negatively stained with 2% uranyl acetate. The samples were examined with an FEI Tecnai 12 transmission electron microscope (FEI, Hillsboro, Oregon, USA).

2.8 | Protein abundance quantification and western blot analysis

Protein concentrations of cell lysate and sEV samples were quantified by Pierce BCA Protein Assay Kit (ThermoFisher, USA) and Bradford Assay (Bio-Rad), respectively, as previously described (Lobb et al., 2017). Bovine serum albumin standards ranging from 0.125 to 2.0 mg/ml were utilised to create an appropriate standard curve. Cell lysate and sEV samples were lysed and heated for 5 min at 95°C . Proteins were resolved in SDS-PAGE and transferred to polyvinylidene fluoride membranes as described (Chen et al., 2015). The membranes were then blocked in 5% non-fat powdered milk diluted in PBS plus 0.5% Tween-20 and

probed with the following primary antibodies: mouse anti-HSP70(1:1000) (610608, BD Biosciences), rabbit anti-CD9(1:5000) (ab92726, Abcam), rabbit anti-calnexin (1:2000) (2679S, CST), mouse anti-TSG101(1:800) (SC7964, Santa Cruz), mouse anti-Flotillin-1 (1:1000) (610821, BD Biosciences), rabbit anti-albumin (1:5000) (ab175934, Abcam). Membranes were further incubated with the appropriate secondary antibodies: goat anti-Mouse IgG HRP (1:30,000) (LTS31430, ThermoFisher) and goat anti-Rabbit IgG HRP (1:10,000) (31460, Life Technologies). Protein expression was detected using Biorad ChemiDoc Touch Imaging System and enhanced chemiluminescence reagent (Amersham ECL Select and Prime).

2.9 | EV labelling

Labelling of sEVs with PKH67 lipophilic dye (Sigma-Aldrich, USA) was performed according to the manufacturer's instructions, with slight modifications. Briefly, 2.5 μg of sEV protein was incubated with Diluent C and PKH67 dye for 5 min, and quenched with 10% BSA in filtered PBS. To avoid PKH67 aggregation, free dye aggregates were removed using OptiPrep Density Gradient Medium (Sigma-Aldrich, USA), by centrifugation at $100,000 \times g$ at 4°C for 16 h. Selected fractions were collected and washed with filtered PBS using Amicon Ultra-4 10 kDa centrifugal filter units by centrifugation at $4000 \times g$ at 4°C , using an Allegra X-15R centrifuge, to concentrate the volume to approximately 100 μl .

2.10 | Sample preparation for proteomic analysis

EV samples were thawed on ice and lysed with 100 mM triethylammonium bicarbonate (TEAB) buffer containing 0.5% SDS. The samples were sonicated in a water bath sonicator for 15 min and centrifuged for 5 min ($21,000 \times g$). The supernatant was collected into a fresh tube and protein lysates were reduced by adding dithiothreitol to final concentration of 5 mM and incubating at 45°C for 20 min. Alkylation was carried out by adding iodoacetamide to a final concentration of 20 mM and incubating at room temperature for 10 min in dark. Four volumes of ice-cold acetone was added to the samples and incubated at -20°C for 4 h to facilitate protein precipitation. At the end of 4 h, the tubes were centrifuged at $21,000 \times g$ (4°C) for 15 min and acetone was removed. The protein pellets were air dried and reconstituted in 100 mM TEAB. Sequencing grade trypsin (Promega, WI, USA) was added at a ratio of 1:20 (enzyme:substrate) and digestion was carried out overnight at 37°C . The digested samples were acidified with formic acid (0.1% final concentration) and dried in a speed vac. The peptides were desalted using C-18 STAGE tips and dried.

2.11 | Mass spectrometry data acquisition

The peptides were reconstituted in 0.1% formic acid and peptide estimation was carried out using a NanoDrop. Peptides (1 μg) were analysed on LTQ-Orbitrap Fusion mass spectrometer (Thermo Scientific, Bremen, Germany) interfaced with a nanoAcquity UHPLC (Waters, MA, USA). The peptide samples were first loaded onto a trap column (Waters, Milford, MA, USA) at a flow rate of 5 $\mu\text{l}/\text{min}$ and then resolved on a BEH C18 nanoAcquity column (Waters, Milford, MA, USA). The peptides were resolved using a gradient of 8% to 70% solvent B (0.1% formic acid in acetonitrile) for 45 min using a flow rate of 300 nl/min . The total run time for each sample was 60 min. The mass spectrometry settings were as follows: MS1 Resolution – 60,000; Mass Range – 350–1800 m/z ; AGC Target – $1e6$, Maximum injection time 22 ms. Include charge state – 2–6; Dynamic exclusion – 30 s. MS2: Isolation mode – Quadrupole; Isolation window – 1.2; Activation type – HCD, Collision energy – 30%; AGC target – 50,000, Maximum injection time – 40 ms.

2.12 | Mass spectrometry data processing

The raw files were searched against *Mus musculus* protein database using SequestHT through Proteome Discoverer software suite (version 2.2). The database was downloaded from UniProt and commonly encountered contaminant protein sequences were added. Search parameters included carbamidomethylation of cysteine as a static modification while oxidation of methionine and deamidation of glutamine and asparagine were dynamic modifications. A mass tolerance of 20 ppm and 0.05 Da were allowed for the precursor and fragments, respectively. A false discovery rate cut-off of 1% was used at both the Peptide Spectrum Match and peptide grouping level. Minora feature detector and precursor ion quantifier nodes were used for calculating protein abundance.

2.13 | Image flow cytometry

Based on particle quantification prior to PKH67-staining, 1×10^8 PKH67-labelled particles were stained with either APC-conjugated CD9 (diluted 1:10; #124812, BioLegend, USA) or PE-conjugated CD63 (diluted 1:5; #12-0631-82, eBioscience, USA)

antibodies, for 2 h on ice. Samples were diluted with filtered PBS to 200 μ l before being analysed by Amnis ImageStream^X Mark II Imaging Flow Cytometer (Luminex, USA). The Amnis ImageStream^X Mark II Imaging Flow Cytometer (Luminex, USA) conducted self-calibration using a series of Automated Suite of Systemwide ImageStream^X tests. All data was acquired with 60 \times magnification, 7 μ m core size, low speed and high sensitivity (lasers: 488 nm (100 mW), 642 nm (150 mW) and 785 nm (2 mW)). Analysis of 10,000 images was conducted using Amnis IDEAS Software (Luminex, USA). Only focused images were selected for analysis. Contamination, aggregation and non-specific staining of lipophilic dyes and fluorescence-conjugated antibodies can generate false positive results (Görgens et al., 2019; Mastoridis et al., 2018). Therefore, various negative controls were applied to ensure appropriate gating of particles, including unstained sEVs, PKH67 dye only, antibody (CD9 or CD63) only, PKH67-labelled sEVs, CD9- or CD63-labelled sEVs, and PKH67 dye plus CD9 or CD63 antibody (Figures S1, S2). Images were gated based on size (Mastoridis et al., 2018); negative signalling in channel 01 (brightfield, 430–480 nm); positive signalling in channel 02 (set to PKH67-related fluorescence, 480–560 nm), aspect ratio larger than 0.5, and positive signalling in each of the antibody-related fluorescence channels (channel 11 (640–745 nm) was set for CD9-APC, and channel 03 (560–595 nm) for CD63-PE) (Figures S1–S3). This gating method allowed for the close selection of small, single, PKH67⁺, CD9⁺/CD63⁺ extracellular vesicles. Data analyses were performed using Amnis IDEAS Software (Luminex, USA).

2.14 | Nano-flow cytometry

Purified sEV samples were analysed by the flow nanoanalyser instrument (nanoFCM) equipped with 488 and 640 nm lasers. Fluorescence measurements were calibrated with 250 nm silica nanospheres labelled with fluorochromes at 20 mW laser power, 0.2% SS decay and 1 kPa sampling pressure. Purified sEVs were labelled with 0.25 μ g of PE-conjugated CD9 (#124806, BioLegend, USA) or PE-conjugated CD63 (#143904, BioLegend, USA), for 60 min at room temperature. Fluorescently-labelled samples were washed with PBS and purified with the Optima Max Benchtop Ultracentrifuge at 110,000 \times *g* at 4°C for 30 min, using the TLA 100.3 rotor. Pellets were then resuspended in PBS and measured at 10 mW laser power, 10% SS decay and 1 kPa sampling pressure. To avoid acquisition of false events, positive regions were gated based on a negative control of PBS and the respective fluorescent antibody to adjust for background fluorescence (Figure S4A–D). The majority of the particles (both ultracentrifugation and tangential flow filtration) analysed were within the size range of sEVs (up to 200 nm), confirmed by size distribution analysis (Figure S4E,F). The data was analysed by NF Profession 1.17 software and FlowJo software (v10.8.1).

2.15 | EV-TRACK

We have submitted all relevant data of our experiments to the EV-TRACK knowledgebase (EV-TRACK ID: EV220091) (Van Deun et al., 2017).

2.16 | Statistical analysis

Depending on the type of data, analyses using repeated measures random effects model followed by Tukey's post-hoc HSD test or quantile regression were performed. Quantile regression with $q = 0.5$ to effectively test medians was utilised. Quantile regression is less sensitive to outliers and deviations from normality (Koenker & Hallock, 2001; Portnoy & Koenker, 1997). Purity (particles per microgram of protein) was analysed using a two-way ANOVA with least squares means contrasts between ultracentrifugation and tangential flow filtration isolation methods for each quantification device (TRPS and NTA (Zetaview and Nanosight)). These analyses were done using JMP Pro (version 16.1.0, SAS Institute, Cary, NC USA). For mass spectrometry, a volcano plot was generated by plotting logworth values ($-\log_{10}$ (FDR *p*-values)) versus \log_2 fold-change, based on protein abundance values, to identify markers that were significantly expressed. The FDR values are the *p*-values from two-sample *t*-tests of the log expression levels corrected for multiple comparison controlling the False-Discovery Rate (Benjamini & Hochberg, 1995).

Unless stated otherwise, all experiments were performed in triplicate with a minimum of three independent replicates. *p*-Values < 0.05 were considered statistically significant (**p* < 0.05; ***p* < 0.01; ****p* < 0.001).

3 | RESULTS

3.1 | A 300 kDa filter membrane successfully separates sEVs

For optimisation of the tangential flow filtration-based isolation protocol, three different filters with molecular weight cut-off values of 300, 500 and 1000 kDa were compared. Various factors, including sEV yield, removal of large EVs and the presence of free protein contaminants were evaluated after the samples were subjected to size exclusion chromatography. Using cell conditioned media from HeLa cells, we observed the size distribution of particles retained by the 500 and 1000 kDa membranes to be inconsistent, reflected by the various peaks in comparison to the 300 kDa membrane (Figure 2A–C). The 300 kDa membrane

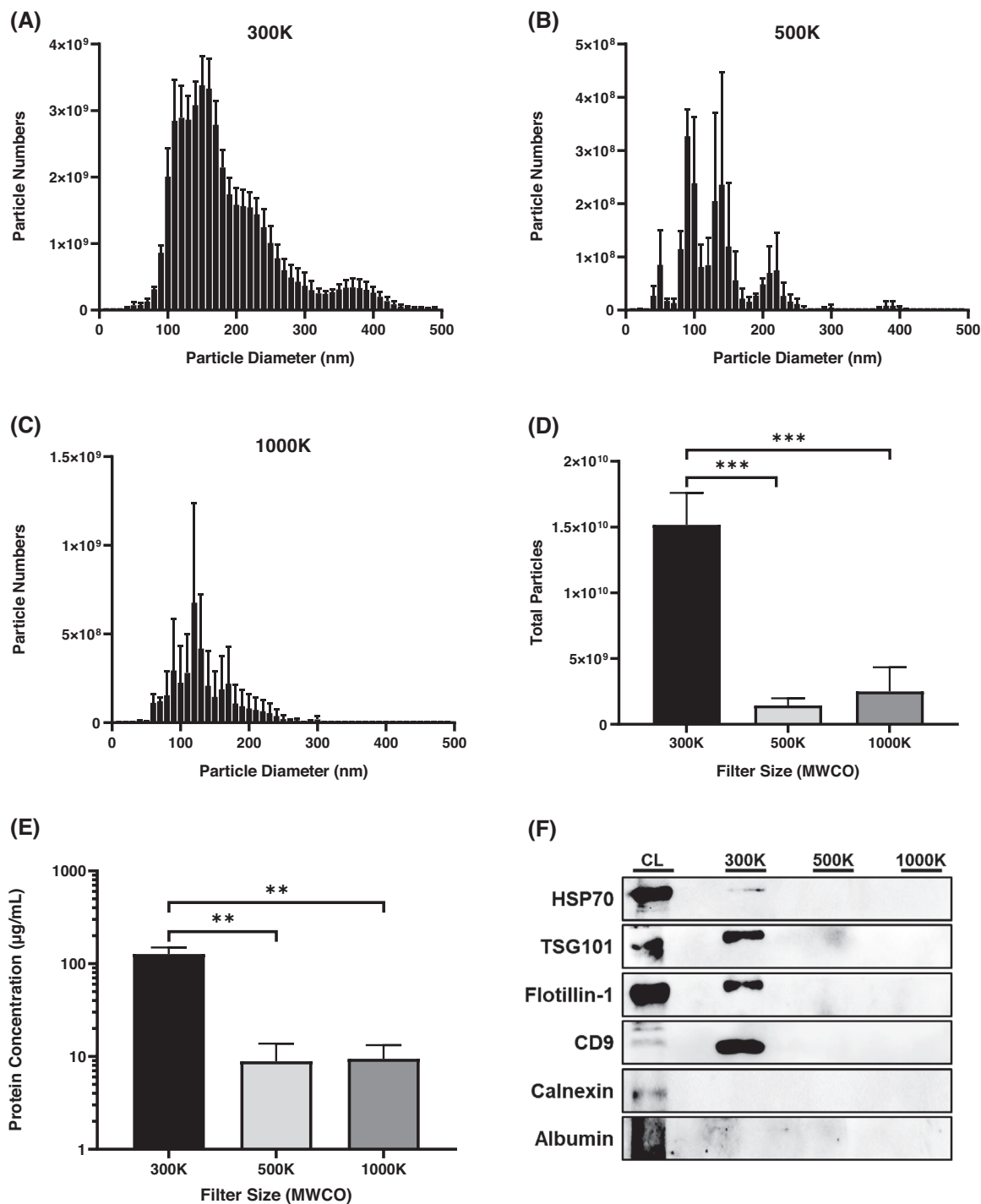


FIGURE 2 Filtration membrane with a molecular weight cut-off of 300 kDa outperformed the 500 and 1000 kDa membranes, for the isolation of sEVs from the human cervical cancer cell line HeLa. (A-C) Size distribution and enumeration of particles and (D) quantification of total particle yield as assessed by Nanoparticle Tracking Analysis. (E) Protein quantification as determined by Bradford Assay. (F) Western blot analysis of sEV markers HSP70, TSG101, Flotillin-1 and CD9 in cell lysate (CL) and sEVs isolated using the different filters. The endoplasmic reticulum marker Calnexin, and the FBS-contaminant Albumin, were also assessed. Equal protein amounts were loaded for each sEV sample. Data are presented as $n = 3 \pm \text{SEM}$. ** $p < 0.01$, *** $p < 0.001$. Statistical analyses were performed using repeated measures random effects model followed by Tukey's post-hoc HSD test, or using quantile regression with $q = 0.5$. CL: cell lysate

retained significantly larger yields of smaller particles, with the total number of particles (<200 nm) being ~10-fold and ~6-fold higher than that of the 500 and 1000 kDa membranes, respectively (Figure 2D). Quantification of protein concentration corroborated the substantial increased yields isolated by the 300 kDa membrane (Figure 2E). For further particle characterisation, equal protein amounts were applied, and sEV protein markers analysed by western blotting. The sEV marker proteins HSP70, TSG101, Flotillin-1 and CD9 were only detected in the 300 kDa sample, suggesting most of the protein detected in the 500 and 1000 kDa isolations to be non-sEV proteins (Figure 2F, Figure S5). Calnexin, an endoplasmic reticulum marker, and Albumin, an FBS protein, were only detected in the cell lysate but not in any of the tangential flow filtration samples (Figure 2F). Based on these findings, we decided to proceed with the 300 kDa membrane as the most appropriate for the isolation of sEVs.

3.2 | Tangential flow filtration produces optimal particle yields from serum-containing cell culture conditioned media in a time-efficient manner, before and after size exclusion chromatography

In comparison to ultracentrifugation, tangential flow filtration reduces time consumption for the isolation of sEVs prior to size exclusion chromatography. Isolating sEVs from 150 ml of HeLa cell culture conditioned media, took a minimum of 130 min using tangential flow filtration, whereas the ultracentrifugation-based method took a minimum of 210 min (Figure S6).

To overcome the lack of uniformity in sEV quantification methods in the literature, three different instruments (qNano, ZetaView and NanoSight) applying two different principles (TRPS and NTA) were employed to quantify particle yields. The TRPS system applies voltage across a membrane containing a pore of a certain size. As particles flow through the pore, the voltage signal is disrupted, altering the duration, magnitude and frequency, which are used to calculate particle concentration and diameter (Anderson et al., 2013; Maas et al., 2015). NTA instruments capture the Brownian motion of individual particles in different fields of view. Using the rate of particle movement, the particle diameter and concentration is calculated (Maas et al., 2015). One of the advantages of ultracentrifugation is its ability to isolate a consistent distribution of particles that fall within a narrow size range (Ayala-Mar et al., 2019; Patel et al., 2019). This advantage is also observed with the tangential flow filtration method, as the size distribution of sEVs isolated by both methods was similar and consistent with profiles of typical sEV preparations (Figure 3A,D,G; Figure S7A,B,D,E,G,H). Tangential flow filtration drastically increased sEV recovery by yielding ~11- to ~27-fold more sEVs (size < 200 nm; yield increase depends on the quantification method applied) than ultracentrifugation (Figure 3B,E,H). Both isolation methods yielded particles within the appropriate sEV size ranges, with the majority being 100 to 200 nm in size (Figure 3C,F,I), peaking at modes between 104 and 123 nm (Figure S7C,F,I).

Size exclusion chromatography is an important step in sEV purification for the separation of sEVs from plasma contaminants (Lobb et al., 2015). Both ultracentrifugation and tangential flow filtration isolates were therefore further purified using size exclusion chromatography. The size distribution of ultracentrifugation and tangential flow filtration sEVs was maintained, corresponding to characteristic sEV profiles (Figure 4A,D,G; Figure S8A,B,D,E,G,H). Tangential flow filtration in combination with size exclusion chromatography resulted in particle (<200 nm) quantities of ~10- to ~20-fold higher than that of ultracentrifugation with subsequent size exclusion chromatography (Figure 4B,E,H). For both approaches, size exclusion chromatography did not alter the size range, with the particles predominantly ranging from 100 to 200 nm in size (Figure 4C,F,I), peaking at modes between 98 and 137 nm (Figure S8C,F,I). Additionally, sEVs isolated by both methods exhibited a round, cup-shaped morphology, which is characteristic for sEVs imaged by transmission electron microscopy (Wu et al., 2015) (Figure 4J,K). Although there is variation in the results produced by the three quantification instruments, all demonstrate a significantly higher sEV recovery by tangential flow filtration compared to ultracentrifugation, after size exclusion chromatography. It is important to note that henceforth, any mention of sEVs isolated by ultracentrifugation or tangential flow filtration, has also undergone size exclusion purification, unless specified otherwise.

One of the requirements for a general sEV preparation protocol is the applicability to a range of cell lines and species. To evaluate if tangential flow filtration generates higher sEV amounts in different cell types, we isolated sEVs from a variety of human and murine cell lines. Irrespective of the cell line, the efficacy of tangential flow filtration in isolating sEVs surpasses ultracentrifugation. For example, for the murine breast cancer line EO771, tangential flow filtration followed by size exclusion chromatography led to ~4-fold more sEVs than ultracentrifugation with size exclusion chromatography (Figure 5A,B, Figure S9A,B). Similarly, there was no impact on the enrichment of particles between 100 and 200 nm in diameter (Figure 5C, Figure S9C). Comparable results were obtained for the human breast cancer cell line MDA-MB-231 (Figure 5D-F, Figure S9D-F), and the murine melanoma cell line B16F10 (Figure 5G-I, Figure S9G-I).

3.3 | Tangential flow filtration combined with size exclusion chromatography recovers sEVs without compromising particle-to-protein ratios

Protein recovery of sEV preparations consists of a combination of sEV proteins and impurities of non-EV proteins. Although tangential flow filtration yielded up to 23-fold higher protein concentration than ultracentrifugation (Figure 6A) after purification

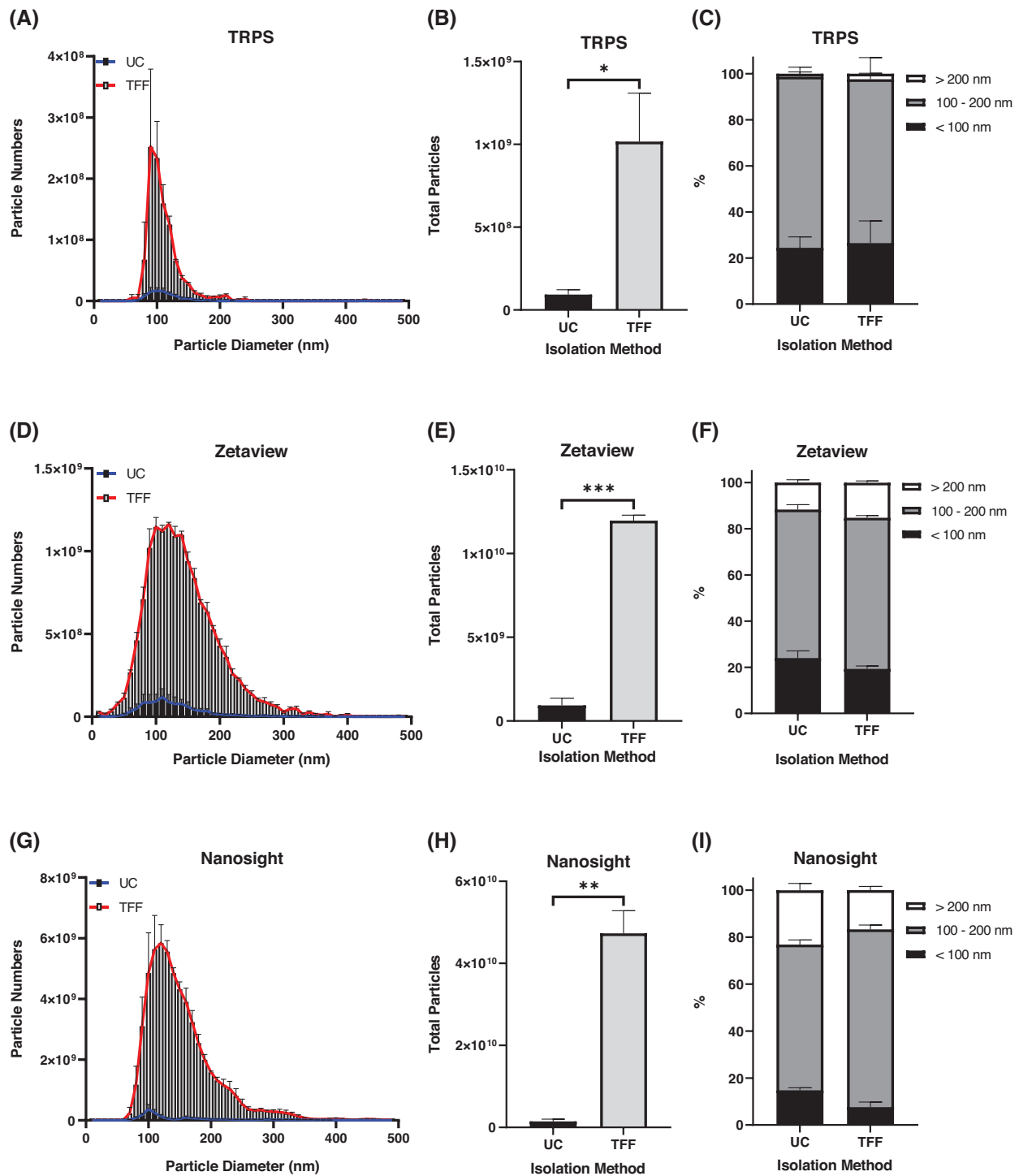


FIGURE 3 Tangential flow filtration isolated significantly higher yields of sEVs from human cervical cancer cell line HeLa, compared to ultracentrifugation, prior to purification by size exclusion chromatography. Size distribution and enumeration of particles, quantification of total particle yield, and percentage of particle size ranges as assessed by (A-C) Tunable Resistive Pulse Sensing (TRPS), (D-F) Zetaview and (G-I) Nanosight. Data are presented as $n = 3 \pm$ SEM. * $p < 0.05$, ** $p < 0.01$, *** $p < 0.001$. Statistical analyses were performed using repeated measures random effects model followed by Tukey's post-hoc HSD test. UC: ultracentrifugation; TFF: tangential flow filtration

by size exclusion chromatography, we cannot conclude that the purity of sEVs is not compromised. Therefore, we employed two ways to determine sEV purity. Firstly, we evaluated sEV proteins CD9, HSP70 and TSG101 in the same number of particles from both isolation methods by western blotting. Assessment of equal particle amounts allows for an accurate representation of protein expression. A marginal increase in the expression of CD9 and TSG101, along with a notable increase in HSP70, was observed in the tangential flow filtration sample (Figure 6B, Figure S10). Intriguingly, assessment of equal protein amounts revealed comparable expression of CD9 and HSP70 between ultracentrifugation and tangential flow filtration (Figure S11A). The endoplasmic

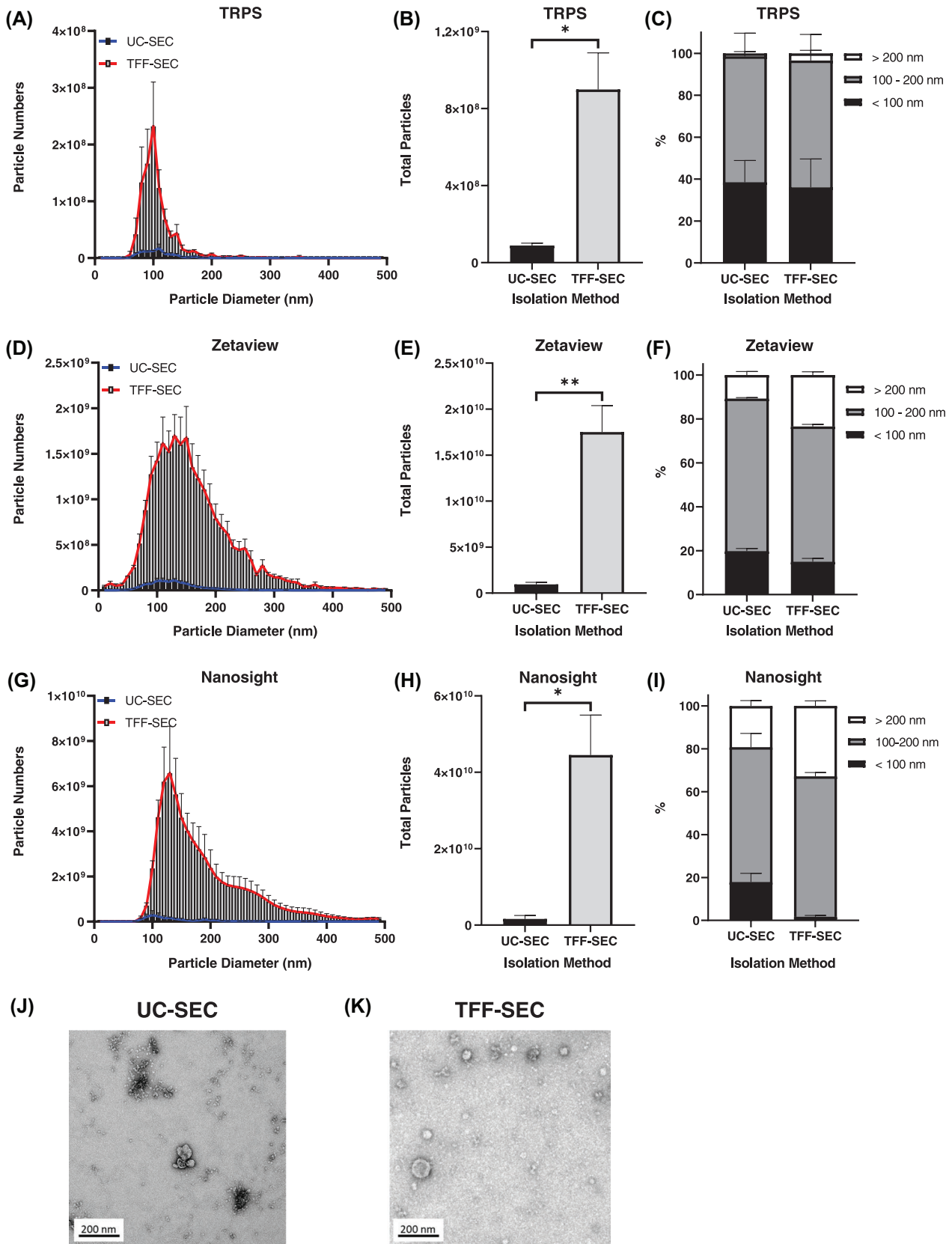


FIGURE 4 Post-size exclusion chromatography purification, the recovery of sEVs from human cervical cancer cell line HeLa, isolated by tangential flow filtration is significantly higher than that of ultracentrifugation. Size distribution and enumeration of particles, quantification of total particle yield, and percentage of particle size ranges as assessed by (A-C) Tunable Resistive Pulse Sensing (TRPS), (D-F) Zetaview and (G-I) Nanosight. Transmission electron microscopy images demonstrated a round, cup-shaped morphology of sEVs isolated by (J) ultracentrifugation and (K) tangential flow filtration. Data are

(Continues)

FIGURE 4 (Continued)

presented as $n = 3 \pm \text{SEM}$. * $p < 0.05$, ** $p < 0.01$. Statistical analyses were performed using repeated measures random effects model followed by Tukey's post-hoc HSD test. UC-SEC: ultracentrifugation-size exclusion chromatography; TFF-SEC: tangential flow filtration-size exclusion chromatography

reticulum marker Calnexin was undetectable in both ultracentrifugation and tangential flow filtration preparations (Figure 6B, Figure S10); however, Calnexin alone is an insufficient measure of purity (Lobb et al., 2015). Albumin was used as an additional purity control as it is the most abundant serum protein (Abramowicz et al., 2018; Baranyai et al., 2015). Both ultracentrifugation and tangential flow filtration contained Albumin, albeit at a higher concentration in tangential flow filtration sEVs (Figure 6B, Figure S10). Interestingly, Albumin was unable to be detected in equal protein amounts of HeLa-derived sEVs isolated by both methods (Figure S11A). Similarly to Figure 6B, Albumin presence in ultracentrifugation and tangential flow filtration sEV preparations was detected in both equal particle and protein amounts of EO771 and B16F10 cell line-derived sEVs. In addition, expression of HSP70 and CD9 were comparable between isolation methods in EO771 and B16F10-derived sEVs (Figure S11B-E). Contrastingly, analysis of the ratio of particles per microgram of protein in the sEV samples isolated by both ultracentrifugation and tangential flow filtration were very similar, regardless of the particle quantification method applied (Figure 6C-E).

3.4 | Ultracentrifugation and tangential flow filtration with subsequent size exclusion chromatography isolate sEVs with slightly different proteomic profiles

The method of isolation can impact the enrichment of specific EV subsets (Brennan et al., 2020; Greening et al., 2015; Patel et al., 2019; Tang et al., 2017). In order to thoroughly evaluate sEV cargo to determine whether tangential flow filtration isolates the same particle subsets as ultracentrifugation, mass spectrometry was conducted on sEVs derived from the EO771 cell line. Proteomic analysis identified 289 sEV proteins. Of the 289 proteins, 61 and 10 were exclusively expressed in sEVs isolated by ultracentrifugation and tangential flow filtration, respectively (Figure 7A, Table S1). The remaining 218 were commonly expressed between both groups (Figure 7A, Table S2). Statistical analysis of the 218 common proteins revealed that with a FDR p -value of 0.05, 1 and 13 proteins were enriched in sEVs isolated by ultracentrifugation and tangential flow filtration, respectively (Figure 7B,C, Table S2). Amongst the 13 tangential flow filtration enriched sEV proteins was ESCRT-III protein Chmp1A (Figure 7B,C, Table S2). Interestingly, the ESCRT-I protein, Mvb12A, and ESCRT-III protein, Chmp2B, were uniquely detected in ultracentrifugation sEVs (Figure 7A, Table S1).

3.5 | sEVs isolated by ultracentrifugation and tangential flow filtration, followed by size exclusion chromatography, express varying levels of CD9

To comprehensively evaluate sEVs prepared by both isolation procedures, analysis of CD9 expression on single, PKH67-labelled EO771-derived sEVs was performed by image flow cytometry. Fluorochrome-conjugated antibodies and lipophilic dyes such as PKH67 have been reported to form sEV-sized aggregates, which can affect sEV analysis (Inglis et al., 2015; Wu et al., 2020). To prevent acquisition of false particles, gating parameters were set based on numerous controls, including unstained sEVs, PKH67 dye only, CD9 antibody only, PKH67 dye plus CD9 antibody, PKH67-labelled sEVs and CD9-labelled sEVs (Figures S1, S3). Analysis of side scatter (channel 06) versus PKH67-related fluorescence (channel 02) allowed for the size-based separation of particles by visual interrogation, based on the unstained sEV control. EVs appear as low scatter/low-mid fluorescence events (G1(EV)), whereas cell debris and large EV aggregates appear as high scatter/high fluorescence events (G2) (Mastoridis et al., 2018) (Figures S1A, S3A,F). From the EV population, using the PKH67-labelled sEV controls, sEVs (G1(sEV)) were gated based on a null brightfield signal (channel 01) and a positive PKH67 signal (channel 02) (Figures S1B, S3B,F). To exclude sEV aggregates, single particles (G1(single sEV)) were gated according to the PKH67-labelled sEV controls, based on aspect ratio values (ratio versus area of PKH67-related fluorescence (channel 02)) larger than 0.5 (Mastoridis et al., 2018). Aspect ratio is indicative of shape and circularity (Jones et al., 2019); thus, due to their round morphology, single sEVs should have mid-high aspect ratio values (Wu et al., 2015) (Figures S1C, S3C,F). Finally, CD9⁺ single sEVs were gated based on the PKH67-labelled sEV controls, for a positive CD9⁺ signal (channel 11) (Figures S1D, S3D,F). Despite the sEV-like aggregates formed by the controls PKH67 dye only and PKH67 dye plus CD9 antibody (Figure S1A-C), CD9 was not detected in the PKH67⁺, CD9⁺ single sEV subset (Figure S1D-G), demonstrating that the gating strategy was effective in eliminating false-positives. In order to bypass the use of PKH67 dye and its associated issues, an additional flow cytometry method, nano-flow cytometry, was employed to assess CD9 expression on sEVs derived from EO771 cells. Nano-flow cytometry is based on a light scattering principle, capable of detecting single particles based on side scatter and fluorescence (Arab et al., 2021). Gating of CD9⁺ regions were based on a PBS plus CD9 antibody negative control (Figure S4A,C), to avoid acquisition of false events. Unlike image flow cytometry, nano-flow cytometry does not require an extensive gating strategy, which evades size-based particle selection. To ensure that the particles analysed were within the sEV size range (up to 200 nm), size distribution profiles were established (Figure S4E,F).

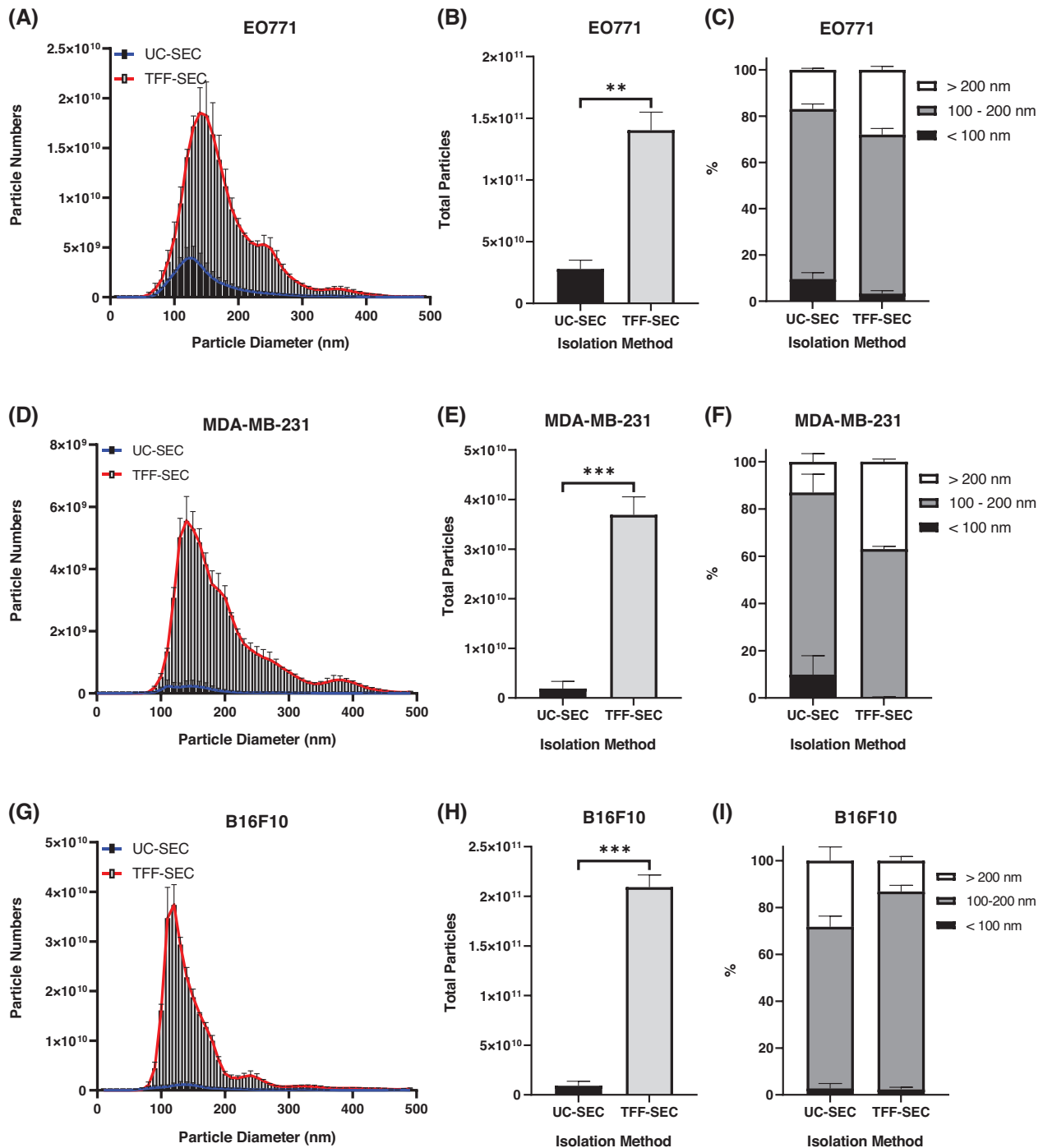


FIGURE 5 Tangential flow filtration effectively isolated significantly higher yields of sEVs from the murine breast cancer cell line EO771, human breast cancer cell line MDA-MB-231 and murine melanoma cell line B16F10, compared to ultracentrifugation. Size distribution and enumeration of particles, quantification of total particle yield, and percentage of particle size ranges from (A-C) EO771, (D-F) MDA-MB-231 and (G-I) B16F10 cell lines, as assessed by Nanoparticle Tracking Analysis. Data are presented as a minimum of $n = 3 \pm \text{SEM}$. ** $p < 0.01$, *** $p < 0.001$. Statistical analyses were performed using quantile regression with $q = 0.5$. UC-SEC: ultracentrifugation-size exclusion chromatography; TFF-SEC: tangential flow filtration-size exclusion chromatography

Assessment of the CD9⁺ single sEV subsets by image flow cytometry (Figure 8A, Figure S12) revealed that 76.2% of ultracentrifugation single sEVs were CD9⁺, significantly higher than the 53.7% of tangential flow filtration single sEVs that were CD9⁺ (Figure 8B). Similarly, the fluorescence intensity of CD9 was significantly higher in ultracentrifugation single sEVs than tangential flow filtration single sEVs (geometric mean of 1206.7 and 508.6, respectively) (Figure 8C). The fluorescence intensity of PKH67 in the CD9⁺ single sEVs was comparable between ultracentrifugation and tangential flow filtration isolation approaches, verifying that the difference in CD9 expression is reflective of sEVs and not of PKH67 aggregates (Figure 8D,E). Interestingly, assessment of CD9⁺ sEVs by nano-flow cytometry (Figure 9A) revealed comparable CD9 expression between ultracentrifugation (28.05%) and tangential flow filtration (30.6%) sEVs (Figure 9B-D).

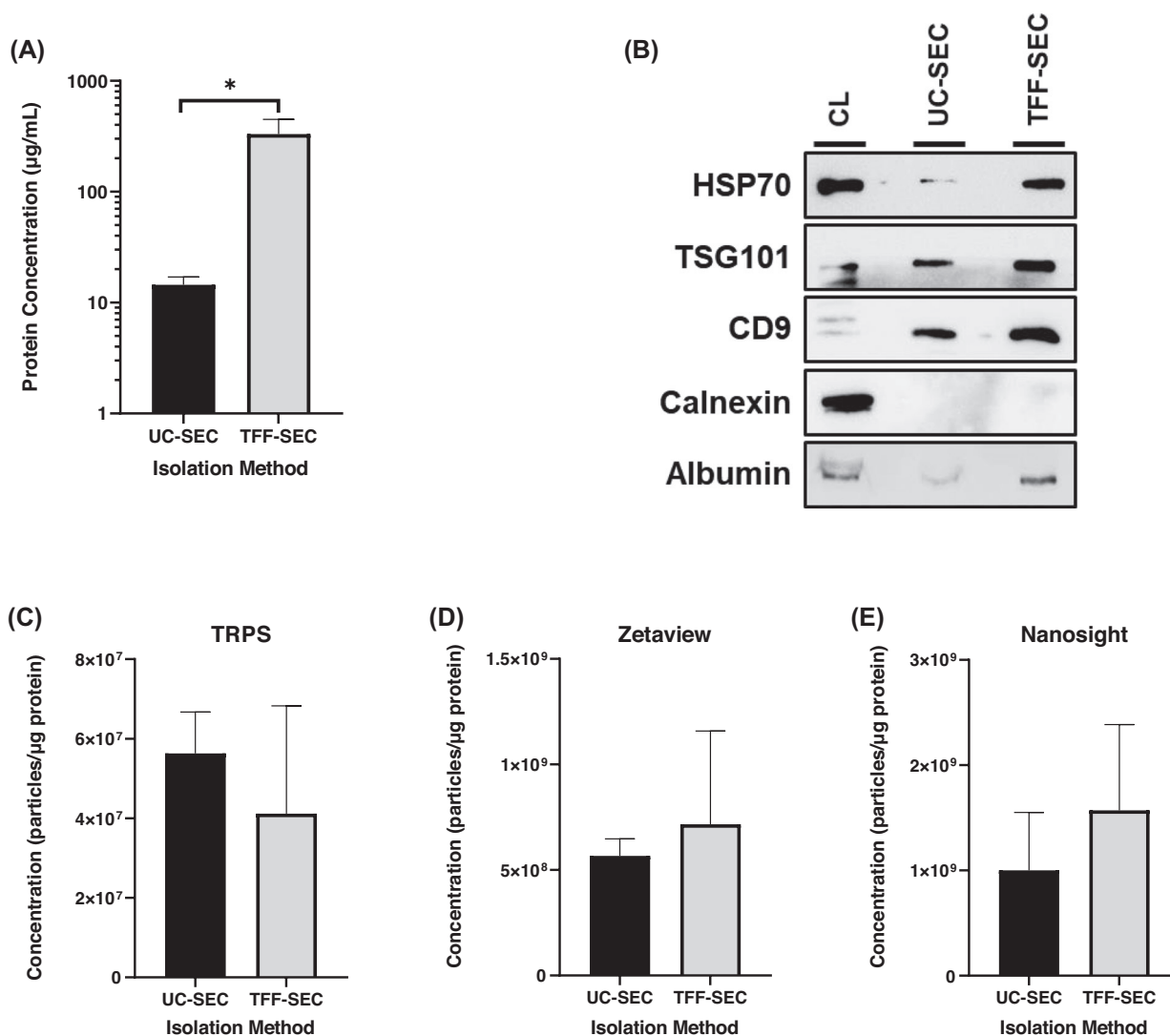


FIGURE 6 After size exclusion chromatography, the purity of particles isolated by ultracentrifugation and tangential flow filtration is comparable. (A) Protein quantification as determined by Bradford Assay. (B) Western blot analysis of sEV markers HSP70, TSG101 and CD9 in cell lysate (CL) and sEVs isolated by ultracentrifugation and tangential flow filtration. The endoplasmic reticulum marker Calnexin, and the FBS-contaminant Albumin, were also assessed. Equal particle amounts (3×10^8 particles) were loaded for each sEV sample. Particle purity expressed as particles per microgram of protein as determined by (C) Tunable Resistive Pulse Sensing (TRPS), (D) Zetaview and (E) Nanosight. Data are presented as $n = 3 \pm$ SEM. * $p < 0.05$. Statistical analyses were performed using quantile regression or two-way ANOVA. UC-SEC: ultracentrifugation-size exclusion chromatography; TFF-SEC: tangential flow filtration-size exclusion chromatography

A similar trend was observed in the analysis of CD63⁺ single sEVs (Figure S13). For image flow cytometry, the frequency of CD63⁺ single sEVs (Figures S13, S14A) was significantly higher in ultracentrifugation (70.6%) than tangential flow filtration (44.4%) (Figure S14B). Although not statistically significant, the fluorescence intensity of CD63 was higher in ultracentrifugation than tangential flow filtration samples, with a geometric mean of 703.6 and 450.3, respectively (Figure S14C), while the fluorescence intensity of PKH67 was comparable (Figure S14D,E). However, due to suboptimal CD63 antibody performance, the controls PKH67 dye only, CD63 antibody only, PKH67 dye plus CD63 antibody, PKH67-labelled sEVs and CD63-labelled sEVs, were positive for CD63 and PKH67, with spill over of the fluorescent signals between channels 02 (set for PKH67-related fluorescence) and channel 03 (set for CD63-PE-related fluorescence) (Figure S2). Similarly to the CD9⁺ sEV subsets, CD63⁺ sEV populations analysed by nano-flow cytometry (Figure S15A), were comparable with 41.5% ultracentrifugation and 33.3% tangential flow filtration sEVs being CD63⁺ (Figure S15B-D).

Together, these data demonstrate several advantages of using tangential flow filtration for the isolation of sEVs, over traditional ultracentrifugation. The ability of tangential flow filtration to isolate substantial, consistent sEV yields makes it the most suitable and compatible method for scalable application. Not only is tangential flow filtration highly reproducible across multiple cell lines and species, but it is also a time-efficient and economical alternative for isolating sEVs from serum-containing media (Table S3).

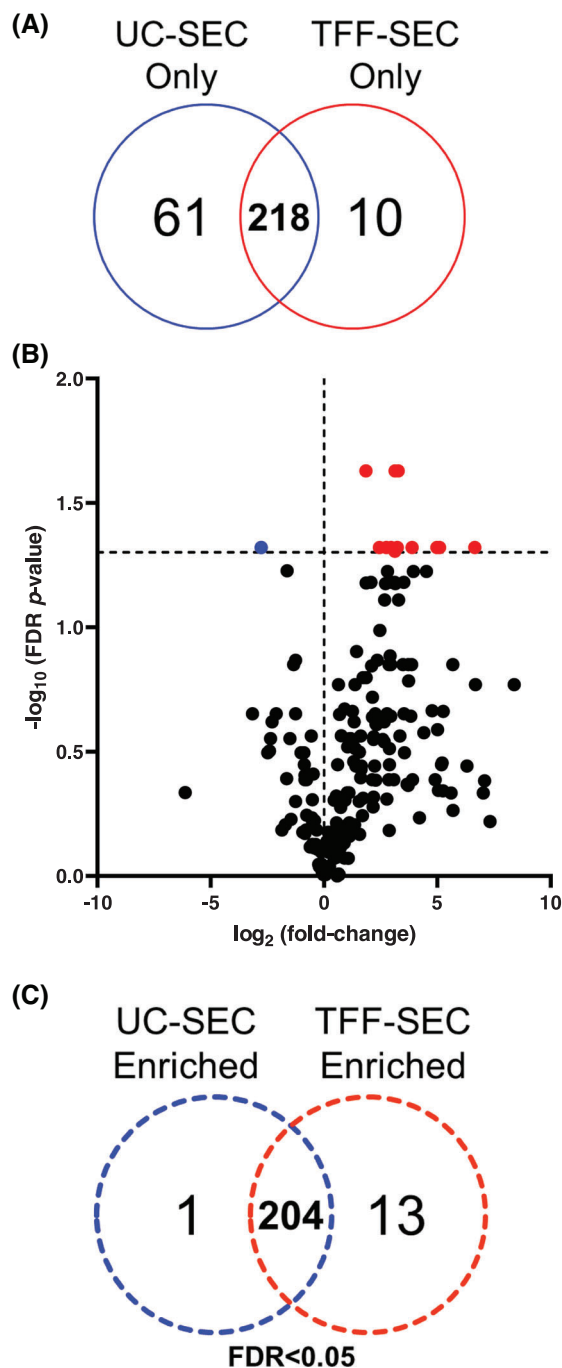


FIGURE 7 Proteomic profiles of UC-SEC and TFF-SEC sEVs slightly differ, as determined by mass spectrometry. sEVs were isolated from the murine breast cancer cell line EO771. (A) Venn diagram of proteins identified in UC-SEC and TFF-SEC sEVs. (B) Volcano plot of 218 proteins commonly expressed in UC-SEC and TFF-SEC sEVs. The horizontal black dotted line corresponds with a significant FDR p -value < 0.05 . Significantly enriched UC-SEC and TFF-SEC sEV proteins are represented as blue and red dots, respectively. (C) Venn diagram of 218 proteins commonly expressed in UC-SEC and TFF-SEC sEVs. UC-SEC: ultracentrifugation-size exclusion chromatography; TFF-SEC: tangential flow filtration-size exclusion chromatography

4 | DISCUSSION

The use of sEVs not only as a tool for clinical or technical applications, but also for our understanding of normal and pathophysiological states, is a rapidly expanding field. However, basic sEV research crucially relies on utilising the most appropriate and robust method of sEV separation. Many researchers use serum-containing media for the conditioning of cells for sEV harvest (Gardiner et al., 2016; Royo et al., 2020; Sciences BCL, 2019) and we therefore require sEV separation methods suitable for these conditions. Ultracentrifugation alone, or in combination with other methods, is the most commonly employed technique for the

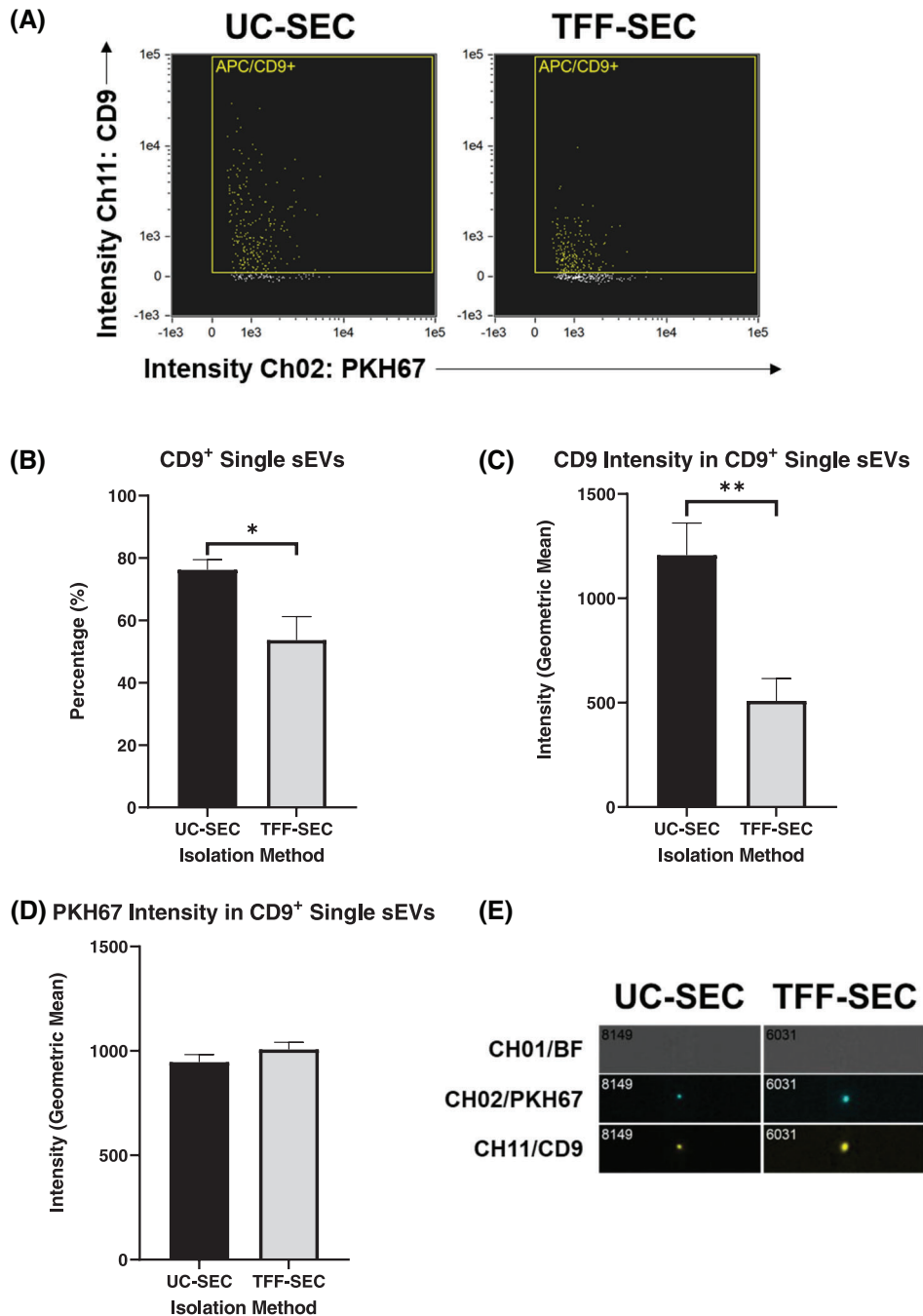


FIGURE 8 Identification and confirmation of the presence of CD9⁺ sEVs in ultracentrifugation and tangential flow filtration samples, as detected by image flow cytometry. sEVs were isolated from the murine breast cancer cell line EO771. Samples were labelled with lipophilic fluorescent dye PKH67, and tagged with fluorescent CD9 (APC) antibody. (A) Dot plot of small, single, PKH67⁺, CD9⁺ EVs. (B) Frequency of CD9⁺ single sEVs. Fluorescence intensity of (C) CD9 and (D) PKH67 in CD9⁺ single sEVs. (E) Images of PKH67-labelled CD9⁺ single sEVs in brightfield (CH01), PKH67-related fluorescence (CH02) and CD9-related fluorescence (CH11) channels. Data are presented as $n = 3 \pm \text{SEM}$. * $p < 0.05$, ** $p < 0.01$. Statistical analyses were performed using quantile regression with $q = 0.5$. UC-SEC: ultracentrifugation-size exclusion chromatography; TFF-SEC: tangential flow filtration-size exclusion chromatography

isolation and purification of sEVs from cell culture media (Gardiner et al., 2016; Royo et al., 2020; Sciences BCL, 2019; Théry et al., 2006; Van Deun et al., 2017). Nonetheless, its use is associated with numerous critical limitations, including low particle recovery, co-isolation of non-EV factors, compromised quality and integrity, high costs and time consumption (Cvjetkovic et al., 2014; Linares et al., 2015; Nordin et al., 2015).

Obtaining reproducibly high yields is one of the many challenges of sEV isolation and is an important factor for large-scale experiments. It is difficult to compare sEV studies due to the numerous quantification methods available and unestablished consensus (Théry et al., 2018). Despite the variability produced by the different instruments, it is clear that tangential flow filtration

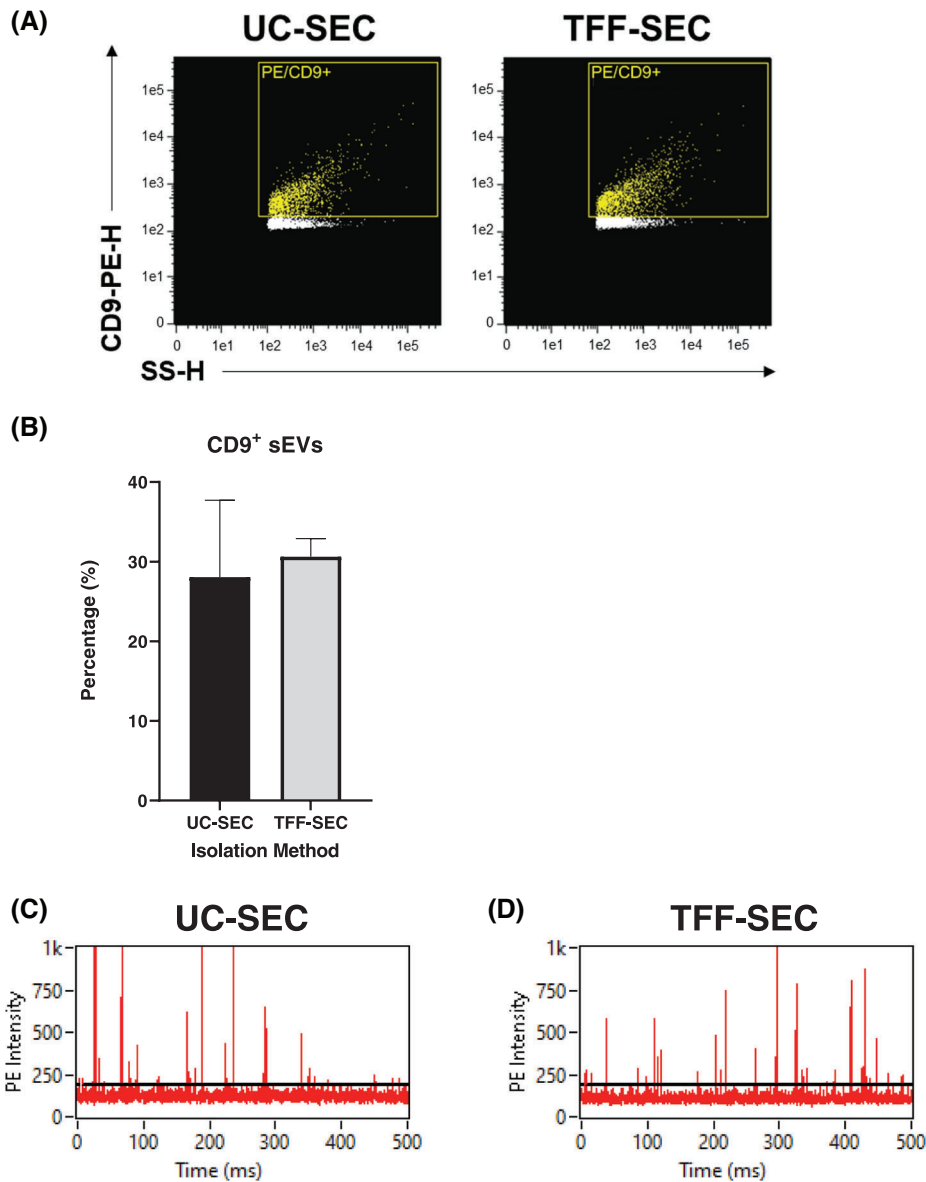


FIGURE 9 Identification and confirmation of the presence of CD9⁺ sEVs in ultracentrifugation and tangential flow filtration samples, as detected by nano-flow cytometry. sEVs were isolated from the murine breast cancer cell line EO771. Samples were tagged with fluorescent CD9 (PE) antibody. (A) Dot plot of CD9⁺ sEVs. (B) Frequency of CD9⁺ sEVs. (C, D) Trace images demonstrating peaks corresponding with CD9 (PE)-related fluorescence. Baseline represents the minimum fluorescence level of any particle detected. Data are presented as $n = 3 \pm \text{SEM}$. Statistical analyses were performed using quantile regression with $q = 0.5$. UC-SEC: ultracentrifugation-size exclusion chromatography; TFF-SEC: tangential flow filtration-size exclusion chromatography

exceeds ultracentrifugation in its ability to maximise sEV yields while maintaining comparable, consistent EV size distribution profiles. One of the advantages of ultracentrifugation is its reliable reproducibility (Konoshenko et al., 2018). Yet tangential flow filtration consistently outperformed ultracentrifugation in isolating substantial sEV quantities from a variety of cancer cell lines of both human and murine species, attesting to its wide-range applicability and reproducibility. Its advantages also imply potential use for the isolation of sEVs from cells conditioned in serum-free media. Previous studies have reported similar findings that tangential flow filtration produced higher sEV quantities than ultracentrifugation (Busatto et al., 2018; Buschmann et al., 2021; El Baradie et al., 2020; Haraszti et al., 2018; Heath et al., 2018; Heinemann et al., 2014; Mcnamara et al., 2018; Watson et al., 2018), as well as findings of comparable size distributions, size ranges and particle diameters between the two isolation methods (El Baradie et al., 2020; Haraszti et al., 2018). Although these previous studies have investigated tangential flow filtration and ultracentrifugation, they have not applied further purification techniques such as size exclusion chromatography and directly compared the combinatorial methods (Busatto et al., 2018; Buschmann et al., 2021; El Baradie et al., 2020; Haraszti et al., 2018; Heath et al., 2018; Heinemann et al., 2014; Mcnamara et al., 2018; Watson et al., 2018).

A major issue associated with the use of serum-containing media is the co-isolation of contaminating materials (Abramowicz et al., 2018). The presence of non-EV structures may affect downstream functional applications and studies, such as proteomics, in vivo experimentation and clinical utility (Abramowicz et al., 2018; Baranyai et al., 2015; Takov et al., 2018), hence the importance of sample purity (Théry et al., 2018). Based on particle-to-protein ratios, overall purity of sEVs isolated by tangential flow filtration and ultracentrifugation is comparable. However, it is important to note that the increased sEV yield produced by tangential flow filtration presumably compensates for the Albumin contamination. Despite that, ultracentrifugation does not effectively remove Albumin either. For downstream applications in which yield is prioritised and Albumin presence does not interfere with analyses, tangential flow filtration is an optimal isolation method. The differing expression levels of sEV markers HSP70, TSG101 and CD9 observed in the ultracentrifugation and tangential flow filtration HeLa samples may be attributed to a difference in the ratio of sEV to non-EV components, such as co-isolation of microvesicles and/or EV fragments. Furthermore, it is feasible that tangential flow filtration isolates different sEV subpopulations to ultracentrifugation. It is noteworthy to mention that differences in HSP70 and CD9 expression were only observed in HeLa sEVs and not in that of B16F10 or EO771 sEVs. This may be attributed to the fact that sEV marker expression is cell-line specific, hence individually impacted by isolation method (Guerreiro et al., 2020; Kowal et al., 2016; Patel et al., 2019), or perhaps western blot lacks the sensitivity to identify minor differences in protein expression between groups.

There are very few studies that have explored the concept of sEV subpopulations. Subgroups separated by size (small (60–80 nm) and large (90–120 nm)) (Zhang et al., 2018), density (low-density (1.12–1.19 g/ml, 75–200 nm) and high-density (1.26–1.29 g/ml, up to 100 nm)) (Willms et al., 2016), and a combination of size and density (low-density-large (1.115 g/ml, larger than 200 nm), low-density-small (1.115 g/ml, up to 200 nm), high-density-large (1.145 g/ml, larger than 200 nm) and high-density-small (1.145 g/ml, up to 200 nm)) (Kowal et al., 2016) have been previously described. Proteomic analysis of the different sEV subsets investigated in these studies revealed comparable expression of TSG101 (Willms et al., 2016; Zhang et al., 2018), CD9, CD63 (Kowal et al., 2016; Willms et al., 2016; Zhang et al., 2018), HSP70 (Kowal et al., 2016) and ESCRT-I (Mvb12A) and ESCRT-III (Chmp1A/2B) components (Kowal et al., 2016; Willms et al., 2016; Zhang et al., 2018) in all subgroups regardless of size and density. Most of the proteins uniquely expressed in ultracentrifugation and tangential flow filtration sEVs have been also been detected in the small, large, low-density and high-density sEVs described in these previous studies, as well as in microvesicles (Kowal et al., 2016; Willms et al., 2016; Zhang et al., 2018) (Tables S4, S5). This suggests that neither ultracentrifugation nor tangential flow filtration enrich or have a bias toward particular sEV subsets. However, the question remains as to why there are a substantial number of proteins only detected in ultracentrifugation sEVs. It is plausible that these unique ultracentrifugation sEV proteins may be associated with non-vesicular particles.

Recent studies have uncovered new subclasses of extracellular nanoparticles termed exomeres and supermeres. Exomeres and supermeres are amembranous particles approximately 35 and 25 nm in size, respectively, with distinct molecular profiles and biophysical characteristics to that of sEVs (Zhang et al., 2018; Zhang et al., 2021). The majority of the proteins exclusively expressed in ultracentrifugation sEVs have also been detected in exomere, supermere and non-vesicular particle populations (Table S4), whereas very few of the unique tangential flow filtration sEV proteins have been detected in these amembranous, non-vesicular subgroups (Table S5) (Zhang et al., 2018; Zhang et al., 2021). Exomeres and supermeres can be isolated by ultracentrifugation, which may explain the high levels of the associated proteins in ultracentrifugation sEVs (Zhang et al., 2021; Zhang et al., 2019). This suggests that tangential flow filtration has higher specificity for isolating sEV particles. However, this can only be confirmed once specific exomere and supermere markers have been established. If tangential flow filtration and ultracentrifugation do isolate different sEV subpopulations, or even non-EV nanoparticles, analysis using additional markers to identify single particles is required.

Examining single sEVs is important for the profiling of sEV subtypes, as there is a large overlap in size range with non-EV contaminants. Although TRPS, NTA and western blot are effective in particle quantification and detecting sEV marker expression, these techniques analyse total vesicle populations, which does not truly represent the heterogeneity of the vesicles isolated (Görgens et al., 2019; Mastoridis et al., 2018; Tertel et al., 2020). Image flow cytometry and nano-flow cytometry were conducted to further characterise ultracentrifugation and tangential flow filtration particles to evaluate the specificity of the isolation technique in selecting for bona fide sEVs. Image and nano-flow cytometry avoid the associated issues of conventional flow cytometry that present when analysing sEVs, such as limited detection thresholds (>500 nm) and background disturbances (Arab et al., 2021; Choi et al., 2019; Lannigan & Erdbruegger, 2017; Mastoridis et al., 2018). These methods offer high fluorescence sensitivity, minimal noise disturbance, clear separation between sEVs and background (Choi et al., 2019; Lannigan & Erdbruegger, 2017), and for image flow cytometry, image confirmation to assess sEVs (Lannigan & Erdbruegger, 2017). However, since sEVs are unable to be detected in brightfield and rely solely on fluorescence, the possibility of aggregates remains (Ricklefs et al., 2019; Yichuan et al., 2020). It has been frequently reported that high-speed ultracentrifugation-based isolation methods cause particle aggregation, loss of particle integrity and formation of particle-like debris due to the shear forces (Cvjetkovic et al., 2014; Linares et al., 2015; Nordin et al., 2015; Théry et al., 2006). Whereas tangential flow filtration applies low pressure and flow rates using cross flow filtration, which in principle is a much more gentle approach than ultracentrifugation, and should avoid excessive exertion or particle manipulation (Heinemann & Vykoukal, 2017). It is plausible that ultracentrifugation samples are contaminated with EV fragments that fall within the PKH67⁺, CD9⁺ single sEV gating, hence impacts image flow cytometry analysis. In addition,

ultracentrifugation-induced particle aggregation may allow for increased antibody binding, hence creates a stronger fluorescent signal, which possibly explains the increase in the fluorescent intensity of CD9⁺ single sEVs isolated by ultracentrifugation compared to tangential flow filtration. On the other hand, the image flow cytometry results may reflect different sEV subpopulations isolated by ultracentrifugation and tangential flow filtration. However, the difference in CD9 expression was not supported by the findings produced by nano-flow cytometry. The conflicting nano-flow cytometry and image flow cytometry results may be ascribed to the absence of lipophilic dye, PKH67. To truly evaluate aggregation caused by these isolation techniques, methods such as cryo-electron microscopy would be required (Yichuan et al., 2020).

An ideal method for sEV isolation should be both time- and cost-efficient. The duration of the ultracentrifugation process is limited by, and dependent on its volume capacity. Larger volumes require additional centrifugation steps and therefore lengthen operation. On the other hand, the time required to execute tangential flow filtration is mostly dependent on sample and buffer flow rates, which is a result of the cell line's particle production. It is to be noted that the larger the sample volume, the slower the flow rate. However, flow rates are consistent and easily maintained using our proposed cleaning protocol, which allows for repeated use of the membrane, thus minimises costs. Ultracentrifugation does not require many reagents or consumables (Konoshenko et al., 2018), as opposed to tangential flow filtration, which requires large volumes of various cleaning buffers. One of the benefits of ultracentrifugation is that it is easy to perform (Li et al., 2017), whereas tangential flow filtration requires various steps and could be considered more difficult to operate. However, these minor limitations are outweighed by the capacity of tangential flow filtration. Tangential flow filtration and subsequent size exclusion chromatography isolates a minimum of 10-fold more particles from HeLa cells than ultracentrifugation followed by size exclusion chromatography. Theoretically, this means that in order to achieve the same sEV yield by ultracentrifugation, it would require a ~10-fold number of cells, cell culture flasks, dishes for sEV harvest, cell growth media, media supplements (FBS and penicillin-streptomycin), PBS, sEV-depleted media and other cell culture-related consumables. As a result, the processing time of ultracentrifugation would increase dramatically, requiring 14 h of ultracentrifugation steps, as opposed to tangential flow filtration, which would only take less than 3 h. Furthermore, ultracentrifugation equipment costs are extraordinarily high, with the combination of benchtop and standing ultracentrifuges, as well as the appropriate tubes and rotors. On the other hand, all materials required for tangential flow filtration, including the pump unit, membranes and ultrafiltration devices, add up to less than one tenth of the equipment costs required for ultracentrifugation. Overall, tangential flow filtration is far more time- and cost-efficient than ultracentrifugation.

With the burgeoning pace of sEV research, establishing a rigorous, reliable and reproducible sEV isolation method that surmounts the numerous problems that the field currently faces, is of high priority. The lack of international consensus delays the progression of sEVs to act as cancer biomarkers for diagnosis and prognosis. Although ultracentrifugation is the most commonly used method worldwide, its multiple disadvantages and limitations are far too great. Using a combination of tangential flow filtration and size exclusion chromatography, we have effectively developed and evaluated a highly effective protocol for the isolation of sEVs from serum-containing cell culture conditioned media and robustly compared it with ultracentrifugation and size exclusion chromatography. Overall, our method isolates significant sEV yields without compromising particle morphology, with high efficiency, specificity and reproducibility. Furthermore, it minimises the use of cell culture-related consumables, saves costs, reduces time consumption and has potential for scalability for downstream applications.

AUTHOR CONTRIBUTIONS

Kekoolani Visan: Conceptualization; Data curation; Formal analysis; Investigation; Methodology; Project administration; Validation; Visualization; Writing—original draft; Writing—review & editing. Richard Lobb: Conceptualization; Data curation; Formal analysis; Methodology; Resources; Validation; Visualization; Writing—original draft; Writing—review & editing. Sun-young Ham: Data curation; Formal analysis; Methodology; Visualization; Writing—original draft; Writing—review & editing. Luize Lima: Data curation; Visualization; Writing—review & editing. Carlos Palma: Formal analysis; Investigation; Writing—review & editing. Edna Chai: Data curation; Investigation; Writing—review & editing. Li-Ying Wu: Data curation; Investigation; Writing—review & editing. Harsha Gowda: Data curation; Formal analysis; Methodology; Writing—original draft; Writing—review & editing. Keshava Datta: Data curation; Formal analysis; Methodology; Writing—original draft; Writing—review & editing. Gunter Hartel: Formal analysis; Methodology; Validation; Writing—original draft; Writing—review & editing. Carlos Salomon: Funding acquisition; Methodology; Writing—original draft; Writing—review & editing. Andreas Möller: Funding acquisition; Project administration; Supervision; Writing—review & editing.

ACKNOWLEDGEMENTS

The authors would like to thank the members of the Tumour Microenvironment Laboratory of QIMR Berghofer Medical Research Institute for critical input and proofreading of the manuscript. We also thank Dr. Sven Kreutel of Particle Metrix for the use of the ZetaView (Particle Metrix, Germany) instrument.

CONFLICT OF INTEREST

The authors report no conflict of interest. This work was funded by grants from the National Health and Medical Research Council Australia (APP1185907) and National Breast Cancer Foundation Australia (IIRS-18-159) to A.M. C.S. is supported by The National Health and Medical Research Council (NHMRC, 1114013).

ORCID

Kekoolani S. Visan  <https://orcid.org/0000-0002-8393-4209>

REFERENCES

- Abramowicz, A., Marczak, L., Wojakowska, A., Zapotoczny, S., Whiteside, T. L., Widlak, P., & Pietrowska, M. (2018). Harmonization of exosome isolation from culture supernatants for optimized proteomics analysis. *Plos One*, *13*(10), e0205496.
- Alameldin, S., Costina, V., Abdel-Baset, H. A., Nitschke, K., Nuhn, P., Neumaier, M., & Hedtke, M. (2021). Coupling size exclusion chromatography to ultracentrifugation improves detection of exosomal proteins from human plasma by LC-MS. *Practical Laboratory Medicine*, *26*, e00241.
- Anderson, W., Kozak, D., Coleman, V. A., Jämting, Å. K., & Trau, M. (2013). A comparative study of submicron particle sizing platforms: Accuracy, precision and resolution analysis of polydisperse particle size distributions. *Journal of Colloid and Interface Science*, *405*, 322–330.
- Andrade, A. C., Wolf, M., Binder, H.-M., Gomes, F. G., Manstein, F., Ebner-Peking, P., Poupardin, R., Zweigerdt, R., Schallmoser, K., & Strunk, D. (2021). Hypoxic conditions promote the angiogenic potential of human induced pluripotent stem cell-derived extracellular vesicles. *International Journal of Molecular Sciences*, *22*(8), 3890.
- Arab, T., Mallick, E. R., Huang, Y., Dong, L., Liao, Z., Zhao, Z., Gololobova, O., Smith, B., Haughey, N. J., Pienta, K. J., Slusher, B. S., Tarwater, P. M., Tosar, J. P., Zivkovic, A. M., Vreeland, W. N., Paulaitis, M. E., & Witwer, K. W. (2021). Characterization of extracellular vesicles and synthetic nanoparticles with four orthogonal single-particle analysis platforms. *Journal of Extracellular Vesicles*, *10*(6), e12079.
- Ayala-Mar, S., Donoso-Quezada, J., Gallo-Villanueva, R. C., Perez-Gonzalez, V. H., & González-Valdez, J. (2019). Recent advances and challenges in the recovery and purification of cellular exosomes. *Electrophoresis*, *40*(23–24), 3036–3049.
- Baranyai, T., Herczeg, K., Onódi, Z., Voszka, I., Módos, K., Marton, N., Nagy, G., Mäger, I., Wood, M. J., El Andaloussi, S., Pálinkás, Z., Kumar, V., Nagy, P., Kittel, Á., Buzás, E. I., Ferdinandy, P., & Giricz, Z. (2015). Isolation of exosomes from blood plasma: Qualitative and quantitative comparison of ultracentrifugation and size exclusion chromatography methods. *Plos One*, *10*(12), e0145686.
- Benjamini, Y., & Hochberg, Y. (1995). Controlling the false discovery rate: A practical and powerful approach to multiple testing. *Journal of the Royal Statistical Society Series B (Methodological)*, *57*(1), 289–300.
- Binder, H.-M., Maeding, N., Wolf, M., Cronemberger Andrade, A., Vari, B., Krisch, L., Gomes, F. G., Blöchl, C., Muigg, K., Poupardin, R., Raninger, A. M., Heuser, T., Obermayer, A., Ebner-Peking, P., Pleyer, L., Greil, R., Huber, C. G., Schallmoser, K., & Strunk, D. (2021). Scalable enrichment of immunomodulatory human acute myeloid leukemia cell line-derived extracellular vesicles. *Cells*, *10*(12), 3321.
- Brennan, K., Martin, K., Fitzgerald, S. P., O'Sullivan, J., Wu, Y., Blanco, A., Richardson, C., & Mc Gee, M. M. (2020). A comparison of methods for the isolation and separation of extracellular vesicles from protein and lipid particles in human serum. *Scientific Reports*, *10*(1), 1039.
- Busatto, S., Vilanilam, G., Ticer, T., Lin, W.-L., Dickson, D., Shapiro, S., Bergese, P., & Wolfram, J. (2018). Tangential flow filtration for highly efficient concentration of extracellular vesicles from large volumes of fluid. *Cells*, *7*(12), 273.
- Buschmann, D., Mussack, V., & Byrd, J. B. (2021). Separation, characterization, and standardization of extracellular vesicles for drug delivery applications. *Advanced Drug Delivery Reviews*, *174*, 348–368.
- Chen, A., Wong, C. S. F., Liu, M. C. P., House, C. M., Sceneay, J., Bowtell, D. D., Thompson, E. W., & Möller, A. (2015). The ubiquitin ligase Siah is a novel regulator of Zeb1 in breast cancer. *Oncotarget*, *6*(2), 862–873.
- Choi, D., Montermini, L., Jeong, H., Sharma, S., Meehan, B., & Rak, J. (2019). Mapping subpopulations of cancer cell-derived extracellular vesicles and particles by nano-flow cytometry. *ACS Nano*, *13*(9), 10499–10511.
- Coenen-Stass, A. M. L., Pauwels, M. J., Hanson, B., Martin Perez, C., Conceição, M., Wood, M. J. A., Mäger, I., & Roberts, T. C. (2019). Extracellular microRNAs exhibit sequence-dependent stability and cellular release kinetics. *RNA Biology*, *16*(5), 696–706.
- Corso, G., Mäger, I., Lee, Y., Görgens, A., Bultema, J., Giebel, B., Wood, M. J. A., Nordin, J. Z., & El Andaloussi, S. (2017). Reproducible and scalable purification of extracellular vesicles using combined bind-elute and size exclusion chromatography. *Scientific Reports*, *7*(1), 11561.
- Cvjetkovic, A., Lötval, J., & Lässer, C. (2014). The influence of rotor type and centrifugation time on the yield and purity of extracellular vesicles. *Journal of Extracellular Vesicles*, *3*(1), 23111.
- Eitan, E., Zhang, S., Witwer, K. W., & Mattson, M. P. (2015). Extracellular vesicle-depleted fetal bovine and human sera have reduced capacity to support cell growth. *Journal of Extracellular Vesicles*, *4*, 26373–.
- El Baradie, K. B. Y., Nouh, M., O'Brien, I. I. F., Liu, Y., Fulzele, S., Eroglu, A., & Hamrick, M. W. (2020). Freeze-dried extracellular vesicles from adipose-derived stem cells prevent hypoxia-induced muscle cell injury. *Frontiers in Cell and Developmental Biology*, *8*, 181.
- Van Deun, J., Mestdagh, P., Agostinis, P., Akay, Ö., Anand, S., Anckaert, J., Martinez, Z. A., Baetens, T., Beghein, E., Bertier, L., Bex, G., Boere, J., Boukouris, S., Bremer, M., Buschmann, D., Byrd, J. B., Casert, C., Cheng, L., Cmoch, A., ... Hendrix, A., EV-TRACK Consortium. (2017). EV-TRACK: Transparent reporting and centralizing knowledge in extracellular vesicle research. *Nature Methods*, *14*(3), 228–232.
- Gardiner, C., Di Vizio, D., Sahoo, S., Théry, C., Witwer, K. W., Wauben, M., & Hill, A. F. (2016). Techniques used for the isolation and characterization of extracellular vesicles: Results of a worldwide survey. *Journal of Extracellular Vesicles*, *5*, 32945.
- Gomes, F. G., Andrade, A. C., Wolf, M., Hochmann, S., Krisch, L., Maeding, N., Regl, C., Poupardin, R., Ebner-Peking, P., Huber, C. G., Meisner-Kober, N., Schallmoser, K., & Strunk, D. (2022). Synergy of human platelet-derived extracellular vesicles with secretome proteins promotes regenerative functions. *Biomedicines*, *10*(2), 238.
- Görgens, A., Bremer, M., Ferrer-Tur, R., Murke, F., Tertel, T., Horn, P. A., Thalmann, S., Welsh, J. A., Probst, C., Guerin, C., Boulanger, C. M., Jones, J. C., Hanenberg, H., Erdbrüggerr, U., Lannigan, J., Ricklefs, F. L., El-Andaloussi, S., & Giebel, B. (2019). Optimisation of imaging flow cytometry for the analysis of single extracellular vesicles by using fluorescence-tagged vesicles as biological reference material. *Journal of Extracellular Vesicles*, *8*(1), 1587567.
- Greening, D. W., Xu, R., Ji, H., Tauro, B. J., & Simpson, R. J. (2015). A protocol for exosome isolation and characterization: Evaluation of ultracentrifugation, density-gradient separation, and immunoaffinity capture methods. In: A. Posch (Ed.), *Proteomic profiling: Methods and protocols* (pp. 179–209). Springer New York.
- Guan, S., Yu, H., Yan, G., Gao, M., Sun, W., & Zhang, X. (2020). Characterization of urinary exosomes purified with size exclusion chromatography and ultracentrifugation. *Journal of Proteome Research*, *19*(6), 2217–2225.

- Guerreiro, E. M., Øvstebø, R., Thiede, B., Costea, D. E., Søland, T. M., Kanli Galtung, H., & Kanli Galtung, H. (2020). Cancer cell line-specific protein profiles in extracellular vesicles identified by proteomics. *PLoS One*, *15*(9), e0238591.
- Ham, S., Lima, L. G., Chai, E. P. Z., Muller, A., Lobb, R. J., Krumeich, S., Wen, S. W., Wiegman, A. P., & Möller, A. (2018). Breast cancer-derived exosomes alter macrophage polarization via gp130/STAT3 signaling. *Frontiers in Immunology*, *9*, 871.
- Haraszti, R. A., Miller, R., Stoppato, M., Sere, Y. Y., Coles, A., Didiot, M.-C., Wollacott, R., Sapp, E., Dubuke, M. L., Li, X., Shaffer, S. A., Difiglia, M., Wang, Y., Aronin, N., & Khvorova, A. (2018). Exosomes produced from 3D cultures of MSCs by tangential flow filtration show higher yield and improved activity. *Molecular Therapy: The journal of the American Society of Gene Therapy*, *26*(12), 2838–2847.
- Heath, N., Grant, L., De Oliveira, T. M., Rowlinson, R., Osteikoetxea, X., Dekker, N., & Overman, R. (2018). Rapid isolation and enrichment of extracellular vesicle preparations using anion exchange chromatography. *Scientific Reports*, *8*(1), 5730.
- Heinemann, M. L., & Vykoukal, J. (2017). Sequential filtration: A gentle method for the isolation of functional extracellular vesicles. In: W. P. Kuo & S. Jia (Eds.), *Extracellular vesicles: Methods and protocols* (pp. 33–41). Springer New York.
- Heinemann, M. L., Ilmer, M., Silva, L. P., Hawke, D. H., Recio, A., Vorontsova, M. A., Alt, E., & Vykoukal, J. (2014). Benchtop isolation and characterization of functional exosomes by sequential filtration. *Journal of Chromatography A*, *1371*, 125–135.
- Inglis, H. C., Danesh, A., Shah, A., Lacroix, J., Spinella, P. C., & Norris, P. J. (2015). Techniques to improve detection and analysis of extracellular vesicles using flow cytometry. *Cytometry Part A: the journal of the International Society for Analytical Cytology*, *87*(11), 1052–1063.
- Jones, P. S., Yekula, A., Lansbury, E., Small, J. L., Ayinon, C., Mordecai, S., Hochberg, F. H., Tigges, J., Delcuze, B., Charest, A., Ghiran, I., Balaj, L., & Carter, B. S. (2019). Characterization of plasma-derived protoporphyrin-IX-positive extracellular vesicles following 5-ALA use in patients with malignant glioma. *EBioMedicine*, *48*, 23–35.
- Kalluri, R., & Lebleu, V. S. (2020). The biology, function, and biomedical applications of exosomes. *Science*, *367*(6478), eaau6977.
- Koenker, R., & Hallock, K. F. (2001). Quantile regression: An introduction. *Journal of Economic Perspectives*, *15*, 143–156.
- Koh, Y. Q., Almughliq, F. B., Vaswani, K., Peiris, H. N., & Mitchell, M. D. (2018). Exosome enrichment by ultracentrifugation and size exclusion chromatography. *Frontiers in Bioscience (Landmark Ed)*, *23*(5), 865–874.
- Konoshenko, M. Y., Lekhnov, E. A., Vlassov, A. V., & Laktionov, P. P. (2018). Isolation of extracellular vesicles: General methodologies and latest trends. *BioMed Research International*, *2018*, 1.
- Kowal, J., Arras, G., Colombo, M., Jouve, M., Morath, J. P., Primdal-Bengtson, B., Dingli, F., Loew, D., Tkach, M., & Théry, C. (2016). Proteomic comparison defines novel markers to characterize heterogeneous populations of extracellular vesicle subtypes. *Proceedings of the National Academy of Sciences*, *113*(8), E968–E977.
- Lamparski, H. G., Metha-Damani, A., Yao, J.-Y., Patel, S., Hsu, D.-H., Ruegg, C., & Le Pecq, J.-B. (2002). Production and characterization of clinical grade exosomes derived from dendritic cells. *Journal of Immunological Methods*, *270*(2), 211–226.
- Lannigan, J., & Erdbruegger, U. (2017). Imaging flow cytometry for the characterization of extracellular vesicles. *Methods (San Diego, Calif.)*, *112*, 55–67.
- Li, J., Lee, Y., Johansson, H. J., Mäger, I., Vader, P., Nordin, J. Z., Wiklander, O. P. B., Lehtiö, J., Wood, M. J. A., & El Andaloussi, S. (2015). Serum-free culture alters the quantity and protein composition of neuroblastoma-derived extracellular vesicles. *Journal of Extracellular Vesicles*, *4*(1), 26883.
- Li, P., Kaslan, M., Lee, S. H., Yao, J., & Gao, Z. (2017). Progress in exosome isolation techniques. *Theranostics*, *7*(3), 789–804.
- Li, X., Corbett, A. L., Taatizadeh, E., Tasnim, N., Little, J. P., Garnis, C., Daugaard, M., Guns, E., Hoorfar, M., & Li, I. T. S. (2019). Challenges and opportunities in exosome research—Perspectives from biology, engineering, and cancer therapy. *APL Bioengineering*, *3*(1), 011503.
- Linares, R., Tan, S., Gounou, C., Arraud, N., & Brisson, A. R. (2015). High-speed centrifugation induces aggregation of extracellular vesicles. *Journal of Extracellular Vesicles*, *4*(1), 29509.
- Lobb, R. J., Becker, M., Wen, S., Wong, C. S. F., Wiegman, A. P., Leimgruber, A., & Möller, A. (2015). Optimized exosome isolation protocol for cell culture supernatant and human plasma. *Journal of Extracellular Vesicles*, *4*, 27031.
- Lobb, R. J., Hastie, M. L., Norris, E. L., Van Amerongen, R., Gorman, J. J., & Möller, A. (2017). Oncogenic transformation of lung cells results in distinct exosome protein profile similar to the cell of origin. *Proteomics*, *17*(23–24), 1600432.
- Maas, S. L. N., De Vrij, J., Van Der Vlist, E. J., Geragousian, B., Van Bloois, L., Mastrobattista, E., Schiffelers, R. M., Wauben, M. H. M., Broekman, M. L. D., & Nolte-T Hoen, E. N. M. (2015). Possibilities and limitations of current technologies for quantification of biological extracellular vesicles and synthetic mimics. *Journal of Controlled Release*, *200*, 87–96.
- Mastoridis, S., Bertolino, G. M., Whitehouse, G., Dazzi, F., Sanchez-Fueyo, A., & Martinez-Llordella, M. (2018). Multiparametric analysis of circulating exosomes and other small extracellular vesicles by advanced imaging flow cytometry. *Frontiers in Immunology*, *9*, 1583.
- Mcnamara, R. P., Caro-Vegas, C. P., Costantini, L. M., Landis, J. T., Griffith, J. D., Damania, B. A., & Dittmer, D. P. (2018). Large-scale, cross-flow based isolation of highly pure and endocytosis-competent extracellular vesicles. *Journal of Extracellular Vesicles*, *7*(1), 1541396.
- Möller, A., House, C. M., Wong, C. S. F., Scanlon, D. B., Liu, M. C. P., Ronai, Z., & Bowtell, D. D. L. (2009). Inhibition of Siah ubiquitin ligase function. *Oncogene*, *28*(2), 289–296.
- Möller, A., & Lobb, R. J. (2020). The evolving translational potential of small extracellular vesicles in cancer. *Nature Reviews Cancer*, *20*(12), 697–709.
- Nordin, J. Z., Bostancioglu, R. B., Corso, G., & El Andaloussi, S. (2019). Tangential flow filtration with or without subsequent bind-elute size exclusion chromatography for purification of extracellular vesicles. In: J. Moll & S. Carotta (Eds.), *Target identification and validation in drug discovery: Methods and protocols* (pp. 287–299). Springer New York.
- Nordin, J. Z., Lee, Y., Vader, P., Mäger, I., Johansson, H. J., Heusermann, W., Wiklander, O. P. B., Hällbrink, M., Seow, Y., Bultema, J. J., Gilthorpe, J., Davies, T., Fairchild, P. J., Gabriellson, S., Meisner-Kober, N. C., Lehtiö, J., Smith, C. I. E., Wood, M. J. A., & El Andaloussi, S. (2015). Ultrafiltration with size-exclusion liquid chromatography for high yield isolation of extracellular vesicles preserving intact biophysical and functional properties. *Nanomedicine: Nanotechnology, Biology and Medicine*, *11*(4), 879–883.
- Patel, G. K., Khan, M. A., Zubair, H., Srivastava, S. K., Khushman, M., Singh, S., & Singh, A. P. (2019). Comparative analysis of exosome isolation methods using culture supernatant for optimum yield, purity and downstream applications. *Scientific Reports*, *9*(1), 5335.
- Portnoy, S., & Koenker, R. (1997). The Gaussian Hare and the Laplacian Tortoise: Computation of squared-error vs. absolute-error estimators. *Statistical Science*, *12*, 279–300.
- Ricklefs, F. L., Maire, C. L., Reimer, R., Dührsen, L., Kolbe, K., Holz, M., Schneider, E., Rissiek, A., Babayan, A., Hille, C., Pantel, K., Krasemann, S., Glatzel, M., Heiland, D. H., Flitsch, J., Martens, T., Schmidt, N. O., Peine, S., Breakefield, X. O., ... Lamszus, K. (2019). Imaging flow cytometry facilitates multiparametric characterization of extracellular vesicles in malignant brain tumours. *Journal of Extracellular Vesicles*, *8*(1), 1588555.
- Royo, F., Théry, C., Falcón-Pérez, J. M., Nieuwland, R., & Witwer, K. W. (2020). Methods for separation and characterization of extracellular vesicles: Results of a worldwide survey performed by the ISEV Rigor and Standardization Subcommittee. *Cells*, *9*(9), 1955.

- Salomon, C., Guanzon, D., Scholz-Romero, K., Longo, S., Correa, P., Illanes, S. E., & Rice, G. E. (2017). Placental exosomes as early biomarker of preeclampsia: Potential role of exosomal MicroRNAs across gestation. *Journal of Clinical Endocrinology and Metabolism*, *102*(9), 3182–3194.
- Salomon, C., Torres, M. J., Kobayashi, M., Scholz-Romero, K., Sobrevia, L., Dobierzewska, A., Illanes, S. E., Mitchell, M. D., & Rice, G. E. (2014). A gestational profile of placental exosomes in maternal plasma and their effects on endothelial cell migration. *Plos One*, *9*(6), e98667.
- Sceneay, J., Chow, M. T., Chen, A., Halse, H. M., Wong, C. S. F., Andrews, D. M., Sloan, E. K., Parker, B. S., Bowtell, D. D., Smyth, M. J., & Möller, A. (2012). Primary tumor hypoxia recruits CD11b+/Ly6Cmed/Ly6G+ immune suppressor cells and compromises NK cell cytotoxicity in the premetastatic niche. *Cancer Research*, *72*(16), 3906–3911.
- Sciences BCL. (2019). Trends in Extracellular Vesicle Research. Accessed on 15 June 2022. <https://www.beckman.es/resources/research-areas/nanoscale/ev-report>
- Stam, J., Bartel, S., Bischoff, R., & Wolters, J. C. (2021). Isolation of extracellular vesicles with combined enrichment methods. *Journal of Chromatography B*, *1169*, 122604.
- Takov, K., Yellon, D. M., & Davidson, S. M. (2018). Comparison of small extracellular vesicles isolated from plasma by ultracentrifugation or size-exclusion chromatography: Yield, purity and functional potential. *Journal of Extracellular Vesicles*, *8*(1), 1560809.
- Tang, Y.-T., Huang, Y.-Y., Zheng, L., Qin, S.-H., Xu, X.-P., An, T.-X., Xu, Y., Wu, Y.-S., Hu, X.-M., Ping, B.-H., & Wang, Q. (2017). Comparison of isolation methods of exosomes and exosomal RNA from cell culture medium and serum. *International Journal of Molecular Medicine*, *40*(3), 834–844.
- Tertel, T., Görgens, A., & Giebel, B. (2020). Chapter Four - Analysis of individual extracellular vesicles by imaging flow cytometry. In: S. Spada & L. Galluzzi (Eds.), *Methods in Enzymology* (Vol. 645, pp. 55–78). Academic Press.
- Théry, C., Amigorena, S., Raposo, G., & Clayton, A. (2006). Isolation and characterization of exosomes from cell culture supernatants and biological fluids. *Current Protocols in Cell Biology*, *30*(1), 3.22.1-3.22.29.
- Théry, C., Witwer, K. W., Aikawa, E., Alcaraz, M. J., Anderson, J. D., Andriantsitohaina, R., Antoniou, A., Arab, T., Archer, F., Atkin-Smith, G. K., Ayre, D. C., Bach, J.-M., Bachurski, D., Baharvand, H., Balaj, L., Baldacchino, S., Bauer, N. N., Baxter, A. A., Bebawy, M., ... Zuba-Surma, E. K. (2018). Minimal information for studies of extracellular vesicles 2018 (MISEV2018): A position statement of the International Society for Extracellular Vesicles and update of the MISEV2014 guidelines. *Journal of Extracellular Vesicles*, *7*(1), 1535750.
- Van der Bruggen, B. (2018). Chapter 2 - Microfiltration, ultrafiltration, nanofiltration, reverse osmosis, and forward osmosis. In: P. Luis (Ed.), *Fundamental modelling of membrane systems* (pp. 25–70). Elsevier.
- Visan, K. S., Lobb, R. J., & Moller, A. (2020). The role of exosomes in the promotion of epithelial-to-mesenchymal transition and metastasis. *Frontiers in Bioscience (Landmark Ed)*, *25*, 1022–1057.
- Visan, K. S., Lobb, R. J., Wen, S. W., Bedo, J., Lima, L. G., Krumeich, S., Palma, C., Ferguson, K., Green, B., Niland, C., Cloonan, N., Simpson, P. T., Mccart Reed, A. E., Everitt, S. J., Macmanus, M. P., Hartel, G., Salomon, C., Lakhani, S. R., Fielding, D., & Möller, A. (2022). Blood-derived extracellular vesicle-associated miR-3182 detects non-small cell lung cancer patients. *Cancers*, *14*(1), 257.
- Watson, D. C., Yung, B. C., Bergamaschi, C., Chowdhury, B., Bear, J., Stellas, D., Morales-Kastresana, A., Jones, J. C., Felber, B. K., Chen, X., & Pavlakis, G. N. (2018). Scalable, cGMP-compatible purification of extracellular vesicles carrying bioactive human heterodimeric IL-15/lactadherin complexes. *Journal of Extracellular Vesicles*, *7*(1), 1442088.
- Wen, S. W., Lima, L. G., Lobb, R. J., Norris, E. L., Hastie, M. L., Krumeich, S., & Möller, A. (2019). Breast cancer-derived exosomes reflect the cell-of-origin phenotype. *Proteomics*, *19*(8), 1800180.
- Willms, E., Johansson, H. J., Mäger, I., Lee, Y., Blomberg, K. E. M., Sadik, M., Alaarg, A., Smith, C. I. E., Lehtiö, J., El Andaloussi, S., Wood, M. J. A., & Vader, P. (2016). Cells release subpopulations of exosomes with distinct molecular and biological properties. *Scientific Reports*, *6*(1), 22519.
- Wolf, M., Poupardin, R. W., Ebner-Peking, P., Andrade, A. C., Blöchl, C., Obermayer, A., Gomes, F. G., Vari, B., Maeding, N., Eminger, E., Binder, H. M., Raninger, A. M., Hochmann, S., Bracht, G., Spittler, A., Heuser, T., Ofir, R., Huber, C. G., Aberman, Z., ... Strunk, D. (2022). A functional corona around extracellular vesicles enhances angiogenesis, skin regeneration and immunomodulation. *Journal of Extracellular Vesicles*, *11*(4), e12207.
- Wu, A. Y., Sung, Y., Chen, Y., Chou, S. T., Guo, V., Chien, J. C., Ko, J. J., Yang, A. L., Huang, H., Chuang, J., Wu, S., Ho, M., Ericsson, M., Lin, W., Cheung, C. H. Y., Juan, H., Ueda, K., Chen, Y., & Lai, C. P. (2020). Multiresolution imaging using bioluminescence resonance energy transfer identifies distinct biodistribution profiles of extracellular vesicles and exomers with redirected tropism. *Advanced science (Weinheim, Baden-Württemberg, Germany)*, *7*(19), 2001467.
- Wu, Y., Deng, W., & Klinken, D. J. 2nd. (2015). Exosomes: Improved methods to characterize their morphology, RNA content, and surface protein biomarkers. *The Analyst*, *140*(19), 6631–6642.
- Yichuan, D., Bai, S., Hu, C., Chu, K., Shen, B., & Smith, Z. (2020). Combined morpho-chemical profiling of individual extracellular vesicles and functional nanoparticles without labels. *Analytical Chemistry*, *92*(7), 5585–5594.
- Zhang, H., Freitas, D., Kim, H. S., Fabijanic, K., Li, Z., Chen, H., Mark, M. T., Molina, H., Martin, A. B., Bojmar, L., Fang, J., Rampersaud, S., Hoshino, A., Matei, I., Kenific, C. M., Nakajima, M., Mutvei, A. P., Sansone, P., Buehring, W., ... Lyden, D. (2018). Identification of distinct nanoparticles and subsets of extracellular vesicles by asymmetric flow field-flow fractionation. *Nature Cell Biology*, *20*(3), 332–343.
- Zhang, Q., Higginbotham, J. N., Jeppesen, D. K., Yang, Y.-P., Li, W., Mckinley, E. T., Graves-Deal, R., Ping, J., Britain, C. M., Dorsett, K. A., Hartman, C. L., Ford, D. A., Allen, R. M., Vickers, K. C., Liu, Q., Franklin, J. L., Bellis, S. L., & Coffey, R. J. (2019). Transfer of functional cargo in exomers. *Cell Reports*, *27*(3), 940–954.e6.
- Zhang, Q., Jeppesen, D. K., Higginbotham, J. N., Graves-Deal, R., Trinh, V. Q., Ramirez, M. A., Sohn, Y., Neining, A. C., Taneja, N., Mckinley, E. T., Niitsu, H., Cao, Z., Evans, R., Glass, S. E., Ray, K. C., Fissell, W. H., Hill, S., Rose, K. L., Huh, W. J., ... Coffey, R. J. (2021). Supermeres are functional extracellular nanoparticles replete with disease biomarkers and therapeutic targets. *Nature Cell Biology*, *23*(12), 1240–1254.

SUPPORTING INFORMATION

Additional supporting information can be found online in the Supporting Information section at the end of this article.

How to cite this article: Visan, K. S., Lobb, R. J., Ham, S., Lima, L. G., Palma, C., Edna, C. P. Z., Wu, L.-Y., Gowda, H., Datta, K. K., Hartel, G., Salomon, C., & Möller, A. (2022). Comparative analysis of tangential flow filtration and ultracentrifugation, both combined with subsequent size exclusion chromatography, for the isolation of small extracellular vesicles. *Journal of Extracellular Vesicles*, *11*, e12266. <https://doi.org/10.1002/jev2.12266>